Angewandte Chemie
Eine Zeitschrift der Gesellschaft Deutscher Chemiker

Supporting Information

EPR Distance Measurements on Long Non-coding RNAs Empowered by Genetic Alphabet Expansion Transcription

Christof Domnick[+], Frank Eggert[+], Christine Wuebben, Lisa Bornewasser, Gregor Hagelueken, Olav Schiemann, and Stephanie Kath-Schorr**

anie_201916447_sm_miscellaneous_information.pdf

Supporting Information

Contents

General Methods

NMR

NMR spectra were recorded using an *Avance dpx 400* from *Bruker*. Chemical shifts (δ) are given in ppm and spectra were calibrated to the respective deuterated solvent residue signal according to literature values ($CDCl_3$: 7.26 ppm for ^1H and 77.2 ppm for ^{13}C spectra, CD_3OD: 3.31 ppm for ^1H and 49.0 ppm for ^{13}C spectra, D_2O: 4.79 ppm for ^1H spectra).[1] Reported coupling constants are calculated from apparent signal positions in first order approximation. Residual peaks in the spectra of nitroxyl-containing compounds correspond to phenylhydrazine.

MS

High resolution (HR) $ESI^{+/-}$ mass spectra were recorded on a *micrOTOF-Q* mass spectrometer from *Bruker Daltonik* or on an *Orbitrap XL* from *Thermo Fisher Scientific*. LC-MS measurements were performed on an *HTC esquire* from *Bruker Daltonik* in combination with an *Agilent 1100* Series HPLC system (*Agilent Technologies*) using a *Zorbax Narrow Bore SB C18* (2.1×50 mm, 5 µm) column (*Agilent Technologies*). As solvent A 10 mM triethylamine/100 mM hexafluoroisopropanol was used for the analysis of oligonucleotides with a gradient of 5 → 20% B in 20 min or 0.1% (*w*/*v*) ammonium acetate for the analysis of triphosphates, respectively (0-60% B in 20 min). In all cases, acetonitrile (MeCN) was used as solvent B.

HPLC

Preparative HPLC purification of triphosphates was carried out on an *Agilent 1200* Series HPLC system (*Agilent Technologies*) in combination with a *Gemini® 5 µm NX-C18 110 Å*, 75×30 mm, *AXIA™* packed column (*Phenomenex*). Used mobile phases and gradients are stated within the corresponding experimental procedure.

HPLC purification of RNA transcripts was performed on an *Agilent 1100* or an *Agilent 1260 Infinity II* Series HPLC system (both from *Agilent Technologies*) with an *EC 150/ 4.6 Nucleodur 100-5 C_{18} ec* column (*Macherey-Nagel*). Gradients used were 0 → 15% B in 15 min with 0.1 M triethylammonium acetate (TEAAc) as solvent A or 0 → 15% B in 30 min with 0.1% NH_4OAc (*w*/*v*) as solvent A, flow rate 1 mL min^{-1}. Acetonitrile was employed as solvent B in both cases.

Chemical Syntheses

TPT3[I] (**3**)[2] and **TPA** (**7**)[3] were synthesized according to literature.

Synthesis of 1-Oxyl-2,2,5,5-tetramethyl-2,5-dihydro-1*H*-pyrrole-3-carboxylic acid prop-2-ynylamide (5)

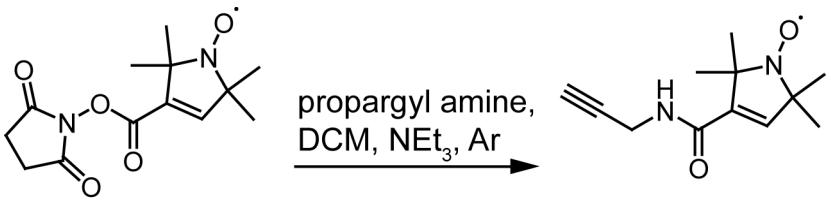

4 **5**

In a flame-dried round bottom flask a mixture of propargylamine (1.5 eq., 3.20 mmol, 0.20 mL) and 1-oxyl-2,2,5,5-tetramethylpyrroline-3-carboxylate (tempyo) *N*-hydroxy-succinimide ester (**4**) (1.0 eq., 2.13 mmol, 600 mg) was dissolved in CH_2Cl_2 (6 mL) under argon atmosphere. After stirring the reaction for two hours at room temperature the colorless precipitate was filtered off and washed with CH_2Cl_2 (2×5 mL). Subsequently the solvent was removed under reduced pressure and the residue was dried *in vacuo*. Product **5** (2.11 mmol, 467 mg, quant.) was quantitatively obtained as yellowish solid.

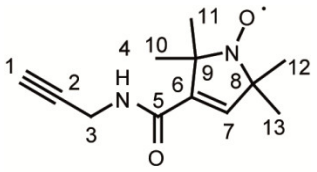

^{1}H-NMR (400 MHz, $CDCl_3$, *in situ* reduced by phenylhydrazine) *δ*: 6.00 (s, 1H, H7), 4.72 (br s, 1H, H4), 3.99 (s, 2H, H3), 2.16 (t, $^4J_{H1H3}$ = 2.3 Hz, 1H, H1), 1.35 (s, 6H, H10, H11, H12, H13), 1.22 (s, 6H, H10, H11, H12, H13).

^{13}C-NMR (101 MHz, $CDCl_3$, *in situ* reduced by phenylhydrazine) *δ*: 163.94 (C5), 140.02 (C6), 137.42 (C7), 129.09 (C8, C9), 128.40, (C8, C9), 79.40 (C2), 71.92 (C1), 29.16 (C3), 24.71 (C10, C11, C12, C13), 24.35 (C10, C11, C12, C13).

HR MS (ESI$^+$): calculated for $[M]^+$: 222.1363; found: *m/z* = 222.1361.

Synthesis of 1-Oxyl-2,2,5,5-tetramethyl-2,5-dihydro-1*H*-pyrrole-3-carboxylic acid (3-(6-(β-D-ribofuranos-1'-yl)-7-thioxo-6,7-dihydrothieno[2,3-*c*]pyridin-4-yl)-prop-2-ynyl)-amide (6)

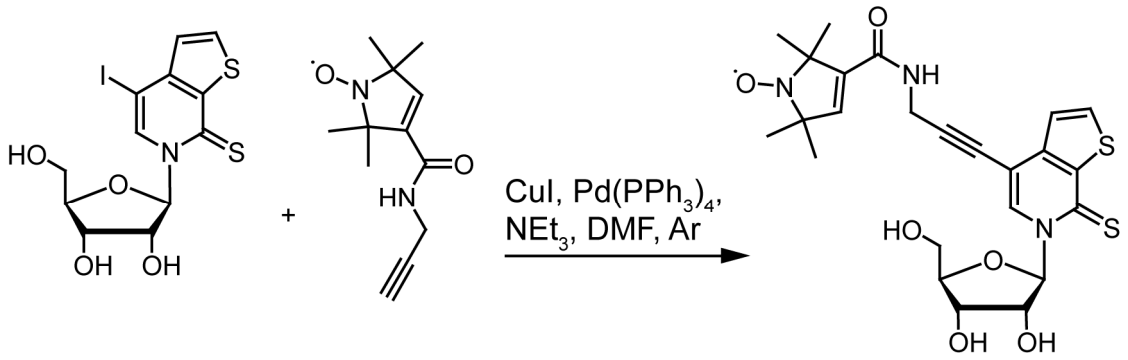

3 **5** **6**

Under an atmosphere of argon **TPT3^{I}** (**3**) (1.0 eq., 0.69 mmol, 295 mg)[2], **5** (1.3 eq., 0.87 mmol, 193 mg), and CuI (0.7 eq., 0.51 mmol, 98 mg) were dissolved in dry DMF (20 mL). The resulting solution was degassed with a stream of argon. Previously degassed NEt_3 (anhydr., 3.0 eq., 2.10 mmol, 213 mg, 0.30 mL) was added subsequently. After the addition of $Pd(PPh_3)_4$ (0.1 eq., 0.07 mmol, 80.9 mg) the mixture was stirred overnight at room temperature under exclusion of light. The solvent was removed *in vacuo* and the residue was purified by column chromatography (CH_2Cl_2/MeOH, 9/1, *v*/*v*). Product **6** (0.47 mmol, 252 mg, 66%) was isolated as beige solid.

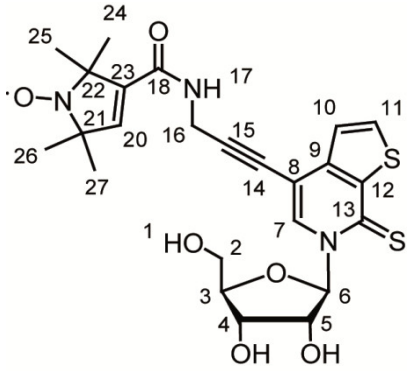

R_f (CH_2Cl_2/MeOH, 9/1, *v*/*v*) = 0.4.

^{1}H-NMR (CD_3OD, 400 MHz, r.t., *in situ* reduced by phenylhydrazine) *δ*: 8.75 (s, 1H, H7), 7.94 (d, $^{3}J_{H11H10}$ = 5.4 Hz, 1H, H11), 7.42 (d, $^{3}J_{H10H11}$ = 5.4 Hz, 1H, H10), 6.89 (d, $^{3}J_{H6H5}$ = 1.4 Hz, 1H, H6), 6.23 (s, 1H, H20), 4.22 (s, 2H, H16), 4.19 (dd, $^{3}J_{H3H4}$ = 4.4 Hz, $^{3}J_{H3H2}$ = 1.6 Hz, 1H, H3), 4.15 – 4.12 (m, 2H, H4, H5), 4.02 (dd, $^{2}J_{H2H2}$ = 12.5 Hz, $^{3}J_{H2H3}$ = 2.0 Hz, 1H, H2), 3.82 (dd, $^{2}J_{H2H2}$ = 12.6 Hz, $^{3}J_{H2H3}$ = 2.3 Hz, 1H, H2), 1.31 (s, 6H, H24, H25, H26, H27), 1.19 (s, 6H, H24, H25, H26, H27).

^{13}C-NMR (CD_3OD, 101 MHz, r.t., *in situ* reduced by phenylhydrazine) *δ*: 174.22 (C13), 167.23 (C18), 145.75 (C12), 140.55 (C23), 139.26 (C11), 135.63 (C7), 129.88 (C8,

C9),124.99 (C10), 105.84 (C14), 96.39 (C6), 91.58 (C15), 85.68 (C3), 71.22 (C2), 60.67 (C1), 30.20 (C16), 25.42 (C24, C25, C26, C27), 25.41 (C24, C25, C26, C27), 25.31 (C24, C25, C26, C27), 25.30 (C24, C25, C26, C27).

HR MS (ESI$^+$): calculated for $[M]^+$: 519.1492; found: *m/z* = 519.1504.

Synthesis of 1-Oxyl-2,2,5,5-tetramethyl-2,5-dihydro-1*H*-pyrrole-3-carboxylic acid (3-(6-(β-D-ribofuranos-5'-triphosphate-1'-yl)-7-thioxo-6,7-dihydrothieno[2,3-*c*]pyridin-4-yl)-prop-2-ynyl)-amide (1, TPT3^{NO} TP)

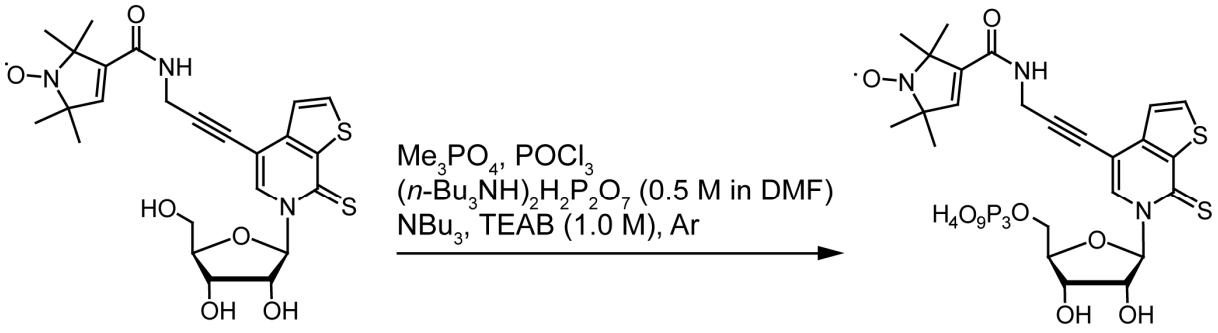

6 **1**

All solutions were freshly prepared or distilled under Argon atmosphere and/or stored over molecular sieve (4 Å). Under an inert atmosphere nucleoside **6** (1.0 eq., 0.15 mmol, 78.0 mg) and proton sponge (1.0 eq., 0.15 mmol, 32.0 mg) were solved in Me_3PO_4 (anhydr., 0.75 mL) and cooled to 0 °C. After the slow addition of $POCl_3$ (2.5 eq., 0.38 mmol, 0.04 mL) the reaction was stirred for 3 h under ice-cold conditions. NBu_3 (10.5 eq., 1.58 mmol, 0.38 mL) and $(n\text{-}Bu_3NH)_2H_2P_2O_7$ (0.5 M in DMF, 5.5 eq., 0.83 mmol, 1.66 mL) were added simultaneously in a rapid manner and the reaction was subsequently stirred for 30 min at 0 °C. The reaction was stopped by the addition of triethylammonium bicarbonate buffer (TEAB, pH 7.0; 1.0 M, 11 mL). The reaction mixture was freeze-dried and triphosphate **1** (**TPT3^{NO}** TP, 0.02 mmol, 21 mg, 13% as 3-fold TEAB salt) was purified by preparative HPLC (0 → 40% B in 6 min; A: 0.1 M TEAB; B: acetonitrile, flow 40 mL min^{-1}) and yielded as colorless solid.

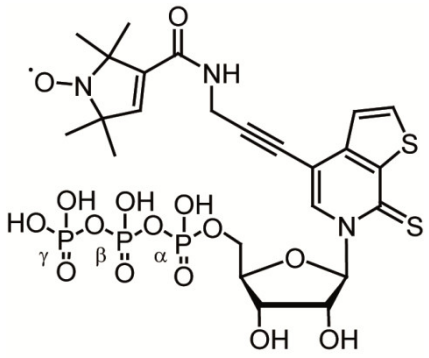

^{31}P-NMR (D_2O, 162 MHz, r.t.) δ: -6.37 (d, $^2J_{P\gamma P\beta}$ = 21.1 Hz, Pγ), -11.54 (d, $^2J_{P\alpha P\beta}$ = 20.4 Hz, Pα), -22.53 (dd, $^2J_{P\beta P\alpha}$ = 20.4 Hz, $^3J_{P\beta P\gamma}$ = 20.4 Hz, Pβ).

HR MS (ESI$^-$): calculated for [M]$^-$: 757.0337; found: *m/z* = 757.0304.

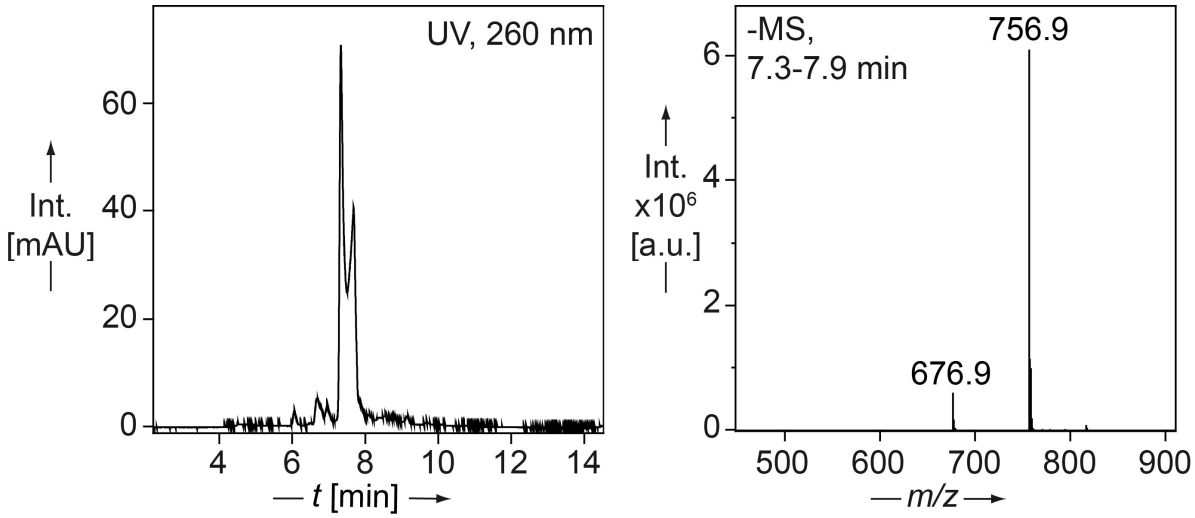

Figure S1. LC-MS analysis of compound **1** (**TPT3^{NO}** TP): UV trace at 260 nm (left panel) and ESI$^-$ mass spectrum (right panel) of the peak eluting at t_R = 7.3-7.9 min (calculated for [M-H]$^-$: 757.0, found *m/z* = 756.9).

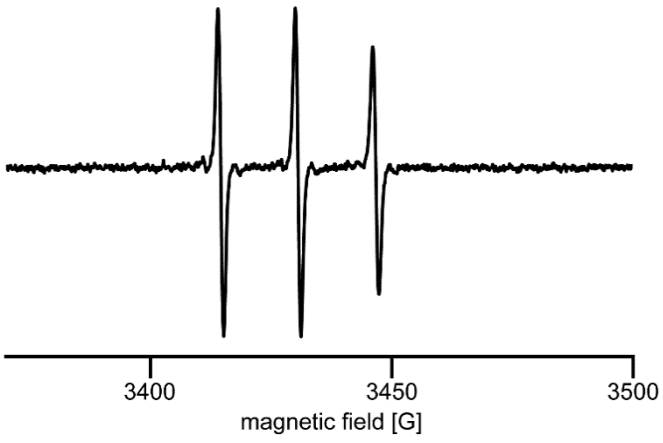

Figure S2. *cw*-X-band EPR of compound **1** in H_2O.

Synthesis of 6-(β-D-ribofuranos-1'-yl)-4-(1-oxyl-2,2,5,5-tetramethyl-2,5-dihydro-1*H*-pyrrol-3-ylethynyl)-6*H*-thieno[2,3-*c*]pyridine-7-thione (8)

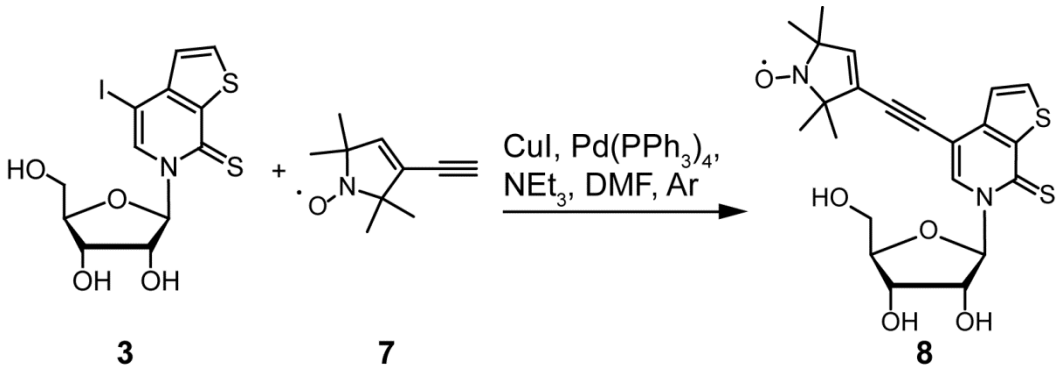

3 **7** **8**

Under an atmosphere of argon **TPT3^{I}** (**3**)[2] (1.0 eq., 0.16 mmol, 68.0 mg), **TPA** (**7**)[3] (1.2 eq., 0.19 mmol, 31.2 mg) and CuI (0.7 eq., 0.11 mmol, 21.0 mg) were dissolved in dry DMF (10 mL) and the resulting solution was degassed with a stream of argon. Previously degassed NEt_3 (anhydr., 3.0 eq., 0.48 mmol, 48.6 mg, 0.07 mL) was added subsequently. After the addition of $Pd(PPh_3)_4$ (0.1 eq., 0.02 mmol, 23.1 mg) the mixture was stirred overnight at room temperature under exclusion of light. The solvent was removed *in vacuo* and the residue was purified by column chromatography (CH_2Cl_2/MeOH, 9/1, *v*/*v*). Product **8** (0.15 mmol, 70.8 mg, 96%) was isolated as yellow solid.

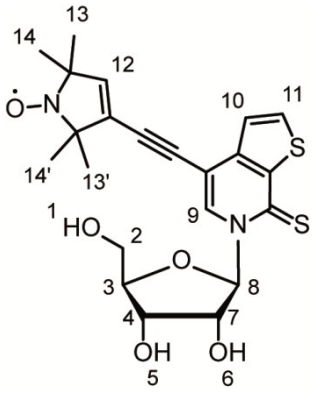

R_f (CH_2Cl_2/MeOH, 9/1, *v*/*v*) = 0.5.

^{1}H-NMR ($CDCl_3$, 400 MHz, r.t., *in situ* reduced by phenylhydrazine) *δ*: 8.44 (s, 1H, H9), 7.76 (d, $^3J_{H11H10}$ = 5.4 Hz, 1H, H11), 7.34 (d, $^3J_{H10H11}$= 5.4 Hz, 1H, H10), 6.78 (d, $^3J_{H8H7}$ = 1.25 Hz, 1H, H8), 5.91 (s, 1H, H12), 4.26 (dd, $^3J_{H3H4}$ = 4.8 Hz, $^3J_{H3H2}$ = 2 Hz, 1H, H3), 4.20 – 4.13 (m, 2H, H4, H7), 4.10 (dd, $^2J_{H2H2}$ = 11.8 Hz, $^3J_{H2H3}$ = 2 Hz, 1H, H2), 3.90 (dd, $^2J_{H2H2}$ = 12.0 Hz, $^3J_{H2H3}$ = 2 Hz, 1H, H2), 1.29 (s, 6H, H13'/14', H13/14), 1.20 (s, 6H, H13/14, H13'/14').

HR MS (ESI$^+$): calculated for $[M]^+$: 461.1205; found; *m/z* = 461.1197.

Synthesis of 6-(β-D-ribofuranos-5'-triphosphate-1'-yl)-4-(1-oxyl-2,2,5,5-tetramethyl-2,5-dihydro-1*H*-pyrrol-3-ylethynyl)-6*H*-thieno[2,3-*c*]pyridine-7-thione (2)

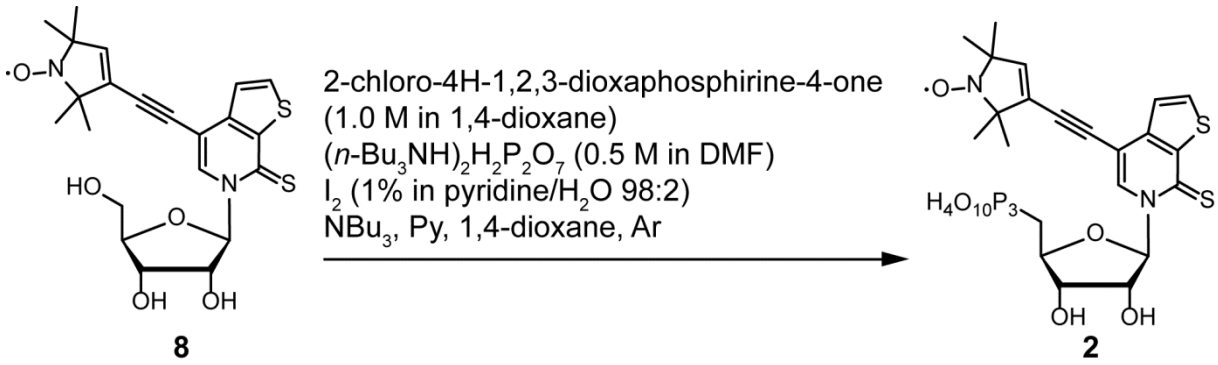

8 **2**

The synthesis was adapted from a procedure described by Marx and coworkers.[4] In an inert atmosphere of argon nucleoside **8** (1.0 eq., 0.24 mmol, 110 mg) was dissolved in pyridine (anhydr., 0.43 mL) and 1,4-dioxane (anhydr., 1.28 mL). At room temperature a solution of 2-chloro-4*H*-1,2,3-dioxaphosphirine-4-one (1.0 M in 1,4-dioxane, anhydr., 1.0 eq., 0.24 mmol, 0.24 mL) was added slowly and the reaction mixture was stirred for 40 min. After the simultaneous addition of NBu_3 (1.0 eq., 0.24 mmol, 0.57 mL) and $(n\text{-}Bu_3NH)_2H_2P_2O_7$ (0.5 M in dry DMF, 1.5 eq., 0.36 mmol, 0.72 mL) the reaction was stirred for additional 40 min. Subsequently an I_2 solution (1% in pyridine/H_2O 98/2, *v*/*v*) was added dropwise until no further discoloration occurred. The excess of iodine was reduced by adding a few drops of an aq. 5% (*m*/*v*) solution of $NaHSO_3$. The solvent was removed under reduced pressure. The crude product was dissolved in H_2O (1 mL) and lyophilized. Purification of **2** (0.01 mmol, 8.41 mg, 5%) was carried out via preparative HPLC (15 → 50% B in 10 min; A: 0.1% NH_4OAc(aq.), B: acetonitrile, flow 40 mL min^{-1}) and the nucleotide was isolated as yellow solid (0.01 mmol, 8.41 mg, 5%).

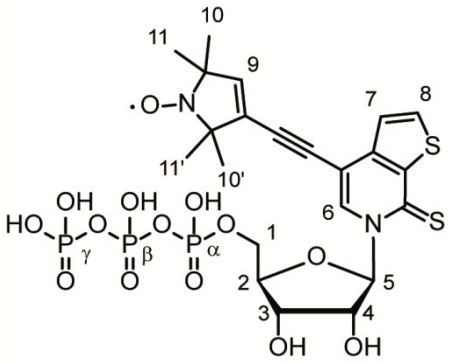

^{31}P-NMR (D_2O, 162 MHz, r.t.) *δ*: -10.24 ($^2J_{P\gamma P\beta}$ = 19.5 Hz, Pγ), -11.95 (d, $^2J_{P\alpha P\beta}$ = 20.3 Hz Hz, Pα), -22.50 (dd, $^2J_{P\beta P\alpha}$ = 20.1 Hz, $^2J_{P\beta P\gamma}$ = 20.1 Hz, Pβ).

^{1}H-NMR (D_2O, 400 MHz, r.t.) *δ*: 8.66 (H6), 7.65 (H7), 7.31 (H8), 6.06 (H5), 5.35 (H9), 5.24 (H3, H4), 4.96 (H3, H4), 4.48 (H2), 3.87 (H1), 3.72 (H1), 1.49 (H10'/11', H10/11), 1.42 (H10/11', H10'/11').

Integrative analysis and determination of coupling constants is not possible due to the paramagnetic spin label and its influence on proton NMR.

HR MS (ESI$^-$): calculated for $[M-2H+Na]^-$: 721.9931; found: *m/z* = 721.9936.

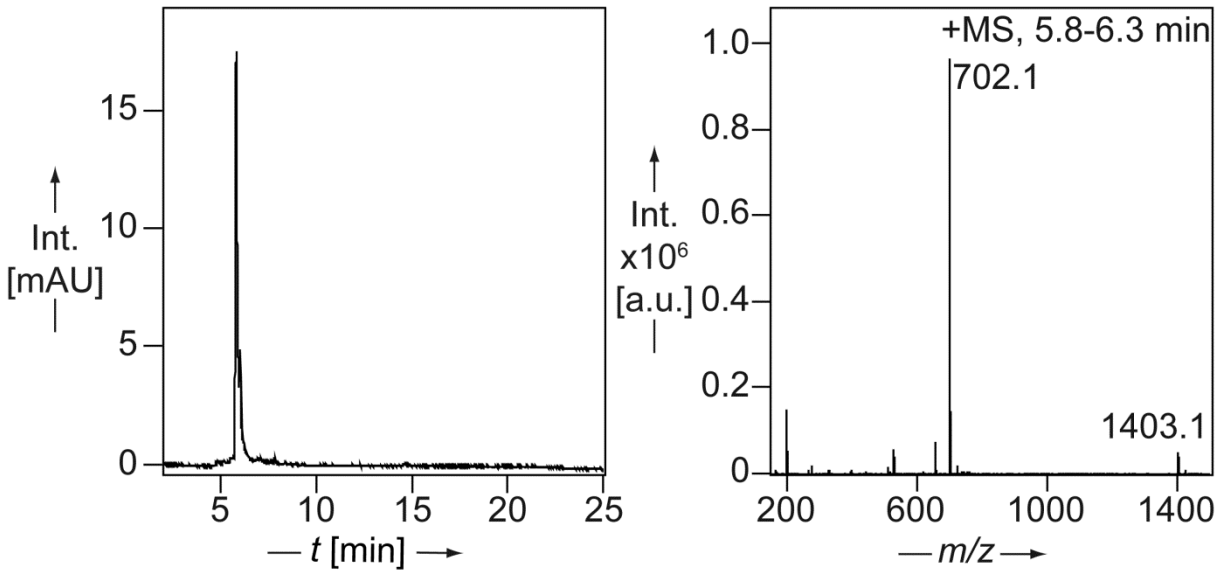

Figure S3. LC-MS analysis of compound **2** (**TPT3^{rNO}** TP): HPL-chromatogram at 260 nm (left panel) and ESI^+ mass spectrum (right panel) of the peak eluting at t_R = 5.8-6.3 min (calculated for $[M+H]^+$: 702.0, found *m/z* = 702.1; $[2M+H]^+$: 1403.1, found *m/z* = 1403.1).

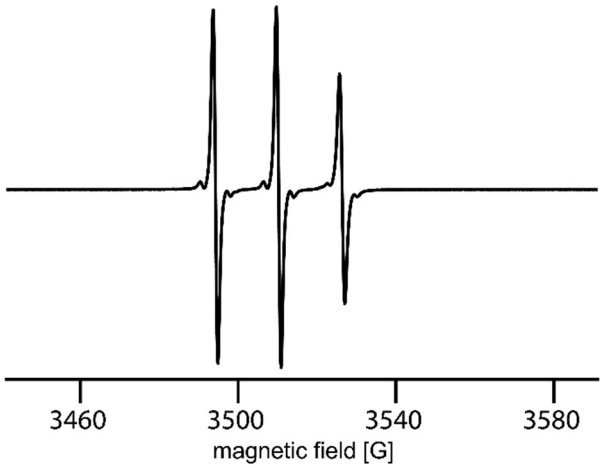

Figure S4. *cw*-X-band EPR of compound **2** in H_2O.

RNA preparation and characterization

Preparation of DNA templates for T7 transcription

d**NaM** nucleoside, d**NaM** cyanoethyl phosphoramidite, and d**5SICS** cyanoethyl phosphoramidite were purchased from *Berry & Associates Inc*., USA. d**TPT3** TP was synthesized according to literature.[5] d**NaM** TP was synthesised from the commercially available nucleoside as described in previous works.[6]

Solid phase syntheses and purification of d**NaM**- and d**5SICS**-modified DNA primers were performed in 200 nmol scale by *Ella Biotech*, Germany. Unmodified DNA primers were synthesized and purified by *Biomers.net*, Germany.

List of DNA and RNA oligonucleotide sequences

A. *Primer for T7 in vitro transcription of self-complementary duplex sequences*

5'-ATA ATA CGA CTC ACT ATA GG-3'

B. *Primer and template strands containing **X** = d**NaM** or **Y** = d**TPT3** or **Z** = d**5SICS***

DNA^{NaM}:

5'-GG**X** TCT GAT ATC AGA TCC TAT AGT GAG TCG TAT TAT-3'

DNA_ext^{NaM}:

5'-GG**X** TCT GAT GCA TCA GAT CCT ATA GTG AGT CGT ATT AT-3'

glmS_3_DNA$^{4–4.1}$:

5'-AGA TCA TGT GAT T**X**C TCT TTG TTC A**X**G GAG TCA CCC CCT TGG TTT GAA GAA ATC CTT ACG GCT GTG-3'

glmS_Pr_RV$^{4–4.1}$:

5'-(MeO-)A(MeO-)GA TCA TGT GAT T**X**C TCT TTG TTC A**X**G G-3'

Xist^{NO}5_3_FW:

5'-TAA TAC GAC TCA CTA TAG GTC CCC GCC A**Z**T CCA TGC-3'

Xist^{NO5}5_3_RV:

5'-(OMe-)A(OMe-)T**X** TCC ATC CAC CAA GCG CCC CG-3'

Xist^{NO}3_3_RV:

5'-(OMe-)A(OMe-)T**X** TCC ATC CAC CA**X** GCG CCC CG-3'

Xist^{NO}5_3 DNA

5'-TAA TAC GAC TCA CTA TAG GTC CCC GCC A**Z**T CCA TGC CCA ACG GGG TTT TGG ATA CTT ACC TGC CTT TTC ATT CTT TTT TTT TCT TAT TAT TTT TTT TTC TAA ACT TGC CCA TCT GGG CTG TGG ATA CCT GCT TTT ATT CTT TTT TTC TTC TCC TTA GCC CAT CGG GGC CAT GGA TAC CTG CTT TTT GTA AAA AAA AAA AAA AAA ACA AAA AAA CCT TTC TCG GTC CAT CGG GAC CTC GGA TAC CTG CGT TTA GTC TTT TTT TCC CAT GCC CAA CGG GGC CTC GGA TAC CTG CTG TTA TTA TTT TTT TTT CTT TTT CTT TTG CCC ATC GGG GCT GTG GAT ACC TGC TTT AAA TTT TTT TTT TCA CGG CCC AAC GGG GCG CTT GGT GGA TGG A**Y**A T-3'

Xist^{NO}3_3 DNA

5'-TAA TAC GAC TCA CTA TAG GTC CCC GCC ATT CCA TGC CCA ACG GGG TTT TGG ATA CTT ACC TGC CTT TTC ATT CTT TTT TTT TCT TAT TAT TTT TTT TTC TAA ACT TGC CCA TCT GGG CTG TGG ATA CCT GCT TTT ATT CTT TTT TTC TTC TCC TTA GCC CAT CGG GGC CAT GGA TAC CTG CTT TTT GTA AAA AAA AAA AAA AAA ACA AAA AAA CCT TTC TCG GTC CAT CGG GAC CTC GGA TAC CTG CGT TTA GTC TTT TTT TCC CAT GCC CAA CGG GGC CTC GGA TAC CTG CTG TTA TTA TTT TTT TTT CTT TTT CTT TTG CCC ATC GGG GCT GTG GAT ACC TGC TTT AAA TTT TTT TTT TCA CGG CCC AAC GGG GCG C**Y**T GGT GGA TGG A**Y**A T-3'

C. *Template strands containing canonical nucleobases*

glmS_1_DNA^{C}:

5'-CCT CCA TCC TCG TCA ACT AAG CCT TTT TCC GGG CGG CTT AGT TCG GGC GCT ATA ATT ATA GGT AAA GCA ATA ATC CTA TAG TGA GTC GTA TTA-3'

glmS_2_DNA^{C}:

5'-AG TTG ACG AGG ATG GAG GTT ATC GAA TTT TCG GCG GAT GCC TCC CGG CTG AGT GTG CAG ATC ACA GCC GTA AGG ATT TCT TC-3'

glmS_3_DNA^{C}:

5'- AGA TCA TGT GAT TTC TCT TTG TTC AAG GAG TCA CCC CCT TGG TTT GAA GAA ATC CTT ACG GCT GTG-3'

glmS_Pr_FW^{C}:

5'-TAA TAC GAC TCA CTA TAG GAT TAT TGC-3'

glmS_Pr_RV^{C}:
5'-AGA TCA TGT GAT TTC TCT TTG TTC-3'

glmS_Pr_RV^{C}_OMe:
5'-(MeO-)A(MeO-)GA TCA TGT GAT TTC TCT TTG TTC -3'

Xist^{NO}3_3_FW:
5'-TAA TAC GAC TCA CTA TAG GTC CCC GCC ATT CCA TGC-3'

*D. RNA transcripts containing either **Y** = r**TPT3**^{NO} or solely canonical nucleobases*
RNA^{NO}:
5'-GGA UCU GAU AUC AGA **Y**CC-3'

RNA^{C}:
5'-GGA UCU GAU AUG AGA UCC-3'

RNA_ext^{NO}:
5'-GGA UCU GAU GCA UCA GA**Y** CC-3'

RNA_ext^{C}:
5'-GGA UCU GAU GCA UCA GAU CC-3'

glmS^{NO}4_4.1:
5'-GGA UUA UUG CUU UAC CUA UAA UUA UAG CGC CCG AAC UAA GCC GCC CGG AAA AAG GCU UAG UUG ACG AGG AUG GAG GUU AUC GAA UUU UCG GCG GAU GCC UCC CGG CUG AGU GUG CAG AUC ACA GCC GUA AGG AUU UCU UCA AAC CAA GGG GGU GAC UCC **Y**UG AAC AAA GAG **Y**AA UCA CAU GAU CU-3'

glmS_RNA^{C} (*B. subtilis*[1]):
5'-GGA UUA UUG CUU UAC CUA UAA UUA UAG CGC CCG AAC UAA GCC GCC CGG AAA AAG GCU UAG UUG ACG AGG AUG GAG GUU AUC GAA UUU UCG GCG GAU GCC UCC CGG CUG AGU GUG CAG AUC ACA GCC GUA AGG AUU UCU UCA AAC CAA GGG GGU GAC UCC UUG AAC AAA GAG AAA UCA CAU GAU CU-3'

[1] Helix P1 was extended by one base pair (additional C added 3' of P1) increasing its stability to allow further modifications in this region.

Xist^{NO}5_3 RNA *(Xist A region nucleotides 365-740)*

5'-G GUC CCC GCC A**Y**U CCA UGC CCA ACG GGG UUU UGG AUA CUU ACC UGC CUU UUC AUU CUU UUU UUU UCU UAU UAU UUU UUU UUC UAA ACU UGC CCA UCU GGG CUG UGG AUA CCU GCU UUU AUU CUU UUU UUC UUC UCC UUA GCC CAU CGG GGC CAU GGA UAC CUG CUU UUU GUA AAA AAA AAA AAA AAA ACA AAA AAA CCU UUC UCG GUC CAU CGG GAC CUC GGA UAC CUG CGU UUA GUC UUU UUU UCC CAU GCC CAA CGG GGC CUC GGA UAC CUG CUG UUA UUA UUU UUU UUU CUU UUU CUU UUG CCC AUC GGG GCU GUG GAU ACC UGC UUU AAA UUU UUU UUU UCA CGG CCC AAC GGG GCG CUU GGU GGA UGG A**Y**A U-3'

Xist^{NO}3_3 RNA *(*Xist A region nucleotides 365-740*)*

5'- G GUC CCC GCC AUU CCA UGC CCA ACG GGG UUU UGG AUA CUU ACC UGC CUU UUC AUU CUU UUU UUU UCU UAU UAU UUU UUU UUC UAA ACU UGC CCA UCU GGG CUG UGG AUA CCU GCU UUU AUU CUU UUU UUC UUC UCC UUA GCC CAU CGG GGC CAU GGA UAC CUG CUU UUU GUA AAA AAA AAA AAA AAA ACA AAA AAA CCU UUC UCG GUC CAU CGG GAC CUC GGA UAC CUG CGU UUA GUC UUU UUU UCC CAU GCC CAA CGG GGC CUC GGA UAC CUG CUG UUA UUA UUU UUU UUU CUU UUU CUU UUG CCC AUC GGG GCU GUG GAU ACC UGC UUU AAA UUU UUU UUU UCA CGG CCC AAC GGG GCG C**Y**U GGU GGA UGG A**Y**A U-3'

E. RNA sequence containing ***Y*** *=* ***TPT3^{rNO}***

RNA^{rNO}:

5'-GGA UCU GAU AUG AGA **Y**CC-3'

PAGE

For analytical (12% or 20%) denaturing PAGE separation, a solution of formamide/8.3 M urea (95/5, *v*/*v*) supplemented with 20 mM ethylenediaminetetraacetic acid (EDTA) was used as loading buffer in equal ratio with the sample volume. Samples were heated to 95 °C for 2 min prior to gel loading. Analytical gels were run at 300 V for 45 min (12%) or 1 h (20%). 1×Tris-borate-EDTA buffer (1×TBE) was employed as running buffer.

Native PAGE (20%) analysis was carried out using 50% glycerol as loading buffer at least in equal ratio to sample volume. Samples were directly loaded on the gel. 1×Tris-borate buffer (1×TB) was employed as running buffer. Gels were run at 60 V for 3 h at 4 °C.

Analytical polyacrylamide gels were stained with *SYBR® Safe* (*Life Technologies)* and visualized by UV illumination using a *Genoplex* gel documentation system (*VWR*).

DNA template preparation

*Fusion PCR approach for the preparation of **glmS_RNA^{C}** and **glmS^{NO}4_4.1** full-length dsDNA templates*

In a first PCR full-length dsDNA was generated from three overlapping DNA fragments as indicated in Figure 1 A, main text. A 100 µL PCR in 1×PCR buffer containing a final concentration of 20 mM Tris-HCl pH 8.9, 22 mM NH_4Cl, 22 mM KCl, 1.8 mM $MgCl_2$, 0.06% IGEPAL® CA-630, 0.05% Tween® 20 (One*Taq*® Standard Reaction Buffer, *New England Biolabs*) supplemented with 1 mM $MgCl_2$, 1 µM templates **glmS_1_DNA^{C}** and **glmS_3_DNA$^{4–4.1/C}$**, 0.5 µM **glmS_2_DNA^{C}**, 375 µM each canonical deoxyribose triphosphate, 0 or 200 µM d**TPT3** TP and d**NaM** TP, and 2.5 U One*Taq*® DNA polymerase (*New England Biolabs*). After 2 min hot start at 95 °C these reactions were submitted to 5 cycles of denaturation at 95 °C for 15 s, 20 s annealing at 57 °C for **glmS_RNA^{C}** and **glmS^{NO}4_4.1** and 1 min elongation at 72 °C.

3 µL of thus obtained dsDNA were submitted to a 100 µL amplification PCR in 1×PCR buffer (see before) supplemented with 1.2 mM $MgCl_2$ for a final concentration of 3.0 mM $MgCl_2$, 2 µM primers **glmS_Pr_FW^{C}** and **glmS_Pr_RV$^{4–4.1/C}$**, 375 µM each canonical deoxyribose triphosphate, 0 or 200 µM d**TPT3** TP and d**NaM** TP, and 2.5 U One*Taq*® polymerase (*New England Biolabs*). Amplification was carried out in 20 cycles of denaturation at 95 °C for 15 s, 20 s annealing at 57 °C (**glmS_RNA^{C}**) or 54 °C (**glmS^{NO}4_4.1**) and 1 min elongation at 72 °C. Optionally, another 2.5 U of One*Taq*® polymerase were added afterwards and the program was repeated.

PCR products were purified with *Nucleospin® Gel and PCR Clean-up kit (Macherey-Nagel*) according to the manufacturers' instructions, eluting the purified DNA into 2×25 µL water.

Six letter PCR approach for the preparation of Xist^{NO}3_3 and Xist^{NO}5_3 DNA templates

The DNA templates for ensuing *in vitro* transcriptions were prepared by PCR amplification of the **Xist lnRNA A region**, in particular nucleotides 426 to 800 of the *pCMV-Xist-PA* plasmid (*Addgene*, #26760) introducing the T7 promotor sequence applying forward primers with a respective overhang sequence and introducing the 3'- and 5'-unnatural base pair modifications applying d**NaM**-modified reverse and d**5SICS**-modified forward primers resulting in either d**NaM**(reverse primer):dT(plasmid) or d**5SICS**(forward primer):dA(plasmid) mismatches.

PCR amplifications were performed in 100 µL scale containing a final concentration of 20 mM Tris HCl pH 8.9, 22 mM NH_4Cl, 22 mM KCl, 1.8 mM MgCl2, 0.06% IGEPAL® CA-630, 0.05% Tween® 20 (*OneTaq*® Standard Reaction Buffer, *New England Biolabs*), 375 µM each canonical dNTP (*Jena Bioscience*), 200 µM d**NaM** TP and d**TPT3** TP, 1 µM forward

and reverse primer (**Xist^{NO}5_3_FW** and **Xist^{NO}5_3_RV** or **Xist^{NO}3_3_FW** and **Xist^{NO}3_3_RV**, respectively), 0.5 ng µL^{-1} *pCMV-Xist-PA* as template and 0.025 U µL^{-1} *OneTaq*® DNA Polymerase (*New England Biolabs*). PCR was performed with an initial denaturing step at 94 °C for 2 min, followed by 30 cycles of denaturing at 94 °C for 30 s, annealing at 54 °C for 40 s for the **Xist^{NO}5_3_FW** and **Xist^{NO}5_3_RV**primer pair or 58 °C for 40 s for the **Xist^{NO}3_3_FW** and **Xist^{NO}3_3_RV** primer pair, respectively, elongation at 68 °C for 1 min, and a final elongation step at 68 °C for 3 min. PCR products were purified using the *NucleoSpin*® Gel and PCR Clean-Up Kit (*Macherey-Nagel*) according to the manufacturers' protocol.

T7 transcription and RNA purification

In vitro transcription

In vitro transcription reactions were prepared in 100 µL scale with final concentrations of 40 mM Tris·HCl pH 7.9 (*Roth*, duplexes and *Xist*) or 40 mM HEPES pH 7.9 (*AppliChem*, glmS constructs), 25 mM $MgCl_2$ (*Alfa Aesar*), 5 mM DTT (*Sigma-Aldrich*), 2.5 mM each canonical triphosphate (*Jena Bioscience*), 0.5 U µL^{-1} RNasin (*Promega*), 3 ng µL^{-1} iPP (*Roche for duplexes* and *New England Biolabs* for glmS and *Xist* constructs), and 5 U µL^{-1} T7 RNA polymerase (*self-made*, AA sequence conforms with GenBank[7]: AY264774.1), which was added to the mixture endmost. Final concentrations of unnatural triphosphates and template DNA will be given in the following for individual experiments:

For self-complementary duplexes **RNA^{NO}** and **RNA_ext^{NO}** a final concentration of 0 or 1 mM **1** or **2** and 3 µM template DNA and primer was used. Template and primer were annealed in buffer containing $MgCl_2$ (95 → 4 °C, cooling rate 5 °C min^{-1}).

For glmS constructs **glmS_RNA^{C}** and **glmS^{NO}4_4.1** a final concentration of 0 or 0.8 mM **1** and 150 nM dsDNA (purified PCR product) was used. In addition, in vitro transcriptions of glmS constructs were supplemented with spermidine with a final concentration of 2 mM

For Xist^{NO}**5_3** and Xist^{NO}**3_3**a final concentration of 5 µg mL^{-1} template **Xist^{NO}5_3 DNA** and template **Xist^{NO}3_3 DNA**, respectively and a final concentration of 0.8 mM **1** was used. Transcriptions were run at 37 °C for 4 h.

Crude reactions were DNase digested by subsequent addition of 12.5 µL 10×DNase I reaction buffer (for duplexes and Xist: 100 mM Tris·HCl pH 7.6, 25 mM $MgCl_2$, 5 mM $CaCl_2$, *New England Biolabs,* for glmS constructs: 100 mM HEPES pH 7.6, 25 mM $MgCl_2$, 5 mM $CaCl_2$, homemade) and RNase-free DNase I (*New England Biolabs*) to a final concentration of 4x10^{-2} U µL^{-1}. Samples were incubated at 37 °C for 30 min, for RNA duplexes followed by enzyme inactivation at 95 °C for 2 min.

*Purification of short RNA duplexes **RNA^{NO}** and **RNA_ex^{NO}***

Crude, DNase-digested transcription reactions of **RNA^{NO}** or **RNA_ext^{NO}** were purified by gel filtration (G-25 columns, *GE Healthcare*) according to the manufacturers' protocol and further purified by RP-HPLC (see general methods).

Purification and characterization of glmS transcripts

Crude, DNase-digested transcription reactions of **glmS_RNA^{C}** and **glmS^{NO}4_4.1** were purified by preparative agarose gel electrophoresis using high resolution agarose (*Carl Roth*) dissolved in 0.5 x TBE (Tris, *Roth*, Boric acid, *Labochem International*, EDTA, *AppliChem*) buffer. Constructs were purified on 2% (w/v) agarose gels with addition of 1 mg mL^{-1} ethidium bromide (*Carl Roth*) at 150 V const. for 15 min, visualized under UV irradiation using a Gel Doc 2000 gel documentation system (*Bio-Rad*), and recovered using NucleoSpin® Gel and PCR Clean-Up Kit (*Macherey-Nagel*) according to the manufacturers' protocol.

For analytical characterization GeneRuler Ultra Low Range DNA Ladder (*Thermo Fisher Scientific*) was used for reference.

Purification and characterization of Xist transcripts

DNase-digested transcription reactions of Xist constructs **Xist^{NO}3_3** and **Xist^{NO}5_3** were purified via preparative agarose gel electrophoresis using high resolution agarose (*Carl Roth*) dissolved in 0.5 x TBE (Tris, *Roth*, Boric acid, *Labochem International*, EDTA, *AppliChem*) buffer. Constructs were purified on 2% (w/v) agarose gels with addition of 1 mg mL^{-1} ethidium bromide (*Carl Roth*) at 150 V const. for 25 min, visualized under UV irradiation using a Gel Doc 2000 gel documentation system (*Bio-Rad*), and recovered using NucleoSpin® Gel and PCR Clean-Up Kit (*Macherey-Nagel*) according to the manufacturers' protocol. Eluates were combined and centrifuged at 18620 x g for 10 min to pellet silica carry-over from the Clean-Up Kit.

For analytical characterization Low Range ssRNA Ladder (*New England Biolabs*) and GeneRuler 100 bp DNA Ladder (*Thermo Fisher Scientific*) were used for reference.

RNA concentration determination

RNA concentration was determined by absorption at 260 nm (A_{260}) using a *Nanodrop* UV-spectrometer *2000c* (*Thermo Fisher Scientific*). Concentrations were obtained from the A_{260} value and software-assisted calculation (native sequences containing canonical bases were plotted for modified RNA or DNA oligonucleotides, *http://biotools.nubic.northwestern.edu/OligoCalc.html*).

*LC-(ESI)-MS of crude RNA transcripts containing **TPT3^{NO}** or **TPT3^{rNO}***

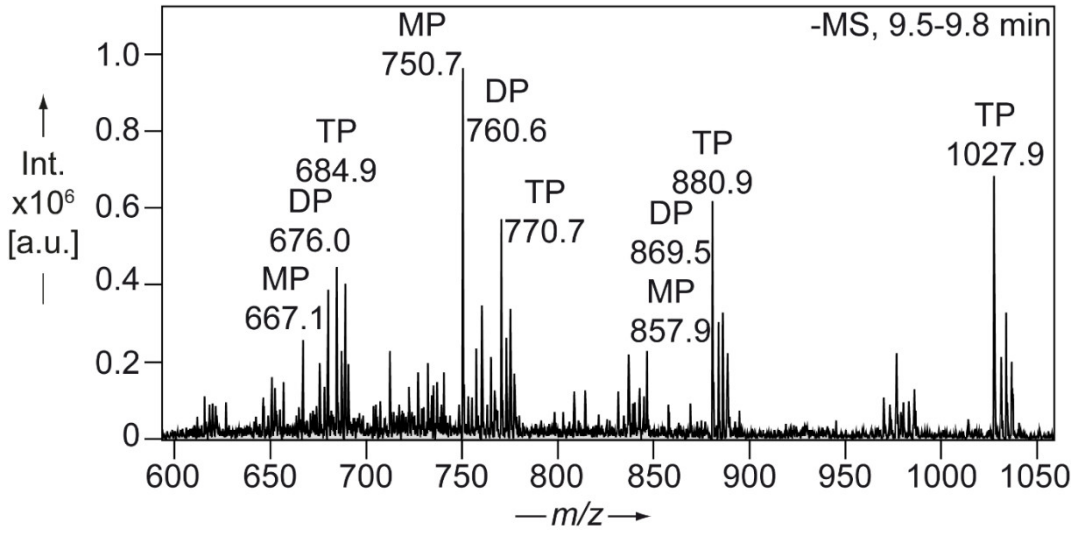

Figure S5. Raw ESI$^-$ traces of spin labeled **RNA^{rNO}** with assigned peaks for 5'-mono- (MP), di- (DP) and triphosphate (TP).

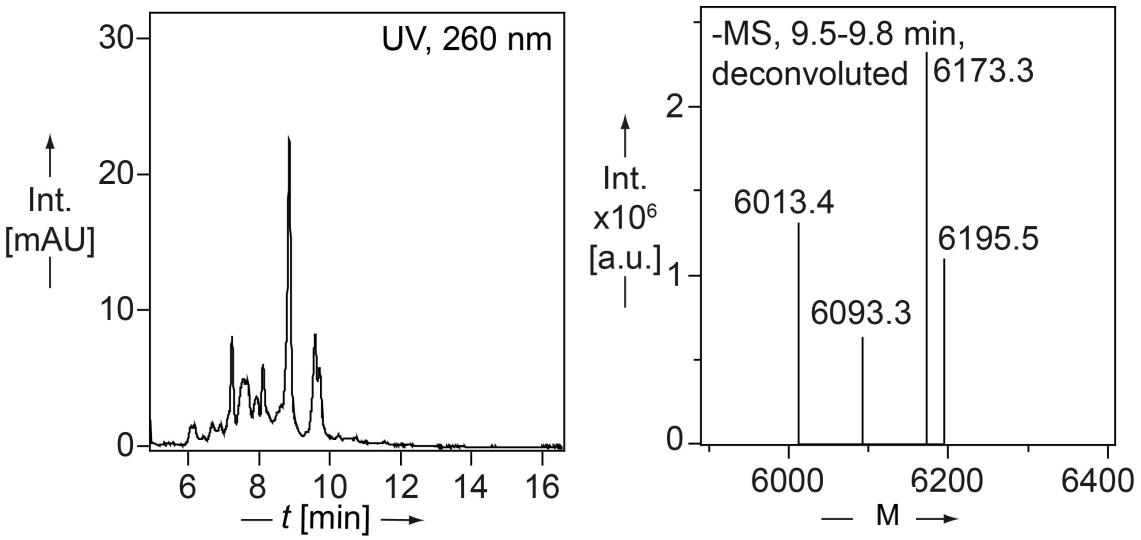

Figure S6. LC-MS analysis showing the UV-trace at 260 nm (left panel) and deconvoluted ESI$^-$ spectrum (right panel) of a crude **RNA^{rNO}** transcription ($M_{calcd.}$ for **RNA^{rNO}**: 5'-MP = 6013.4, found: *m*/*z* = 6013.4; 5'-DP = 6093.4, found: M = 6093.3; 5'-TP = 6173.4, found: M = 6173.3; 5'-TP+Na$^+$ = 6195.3, found: M = 6195.5).

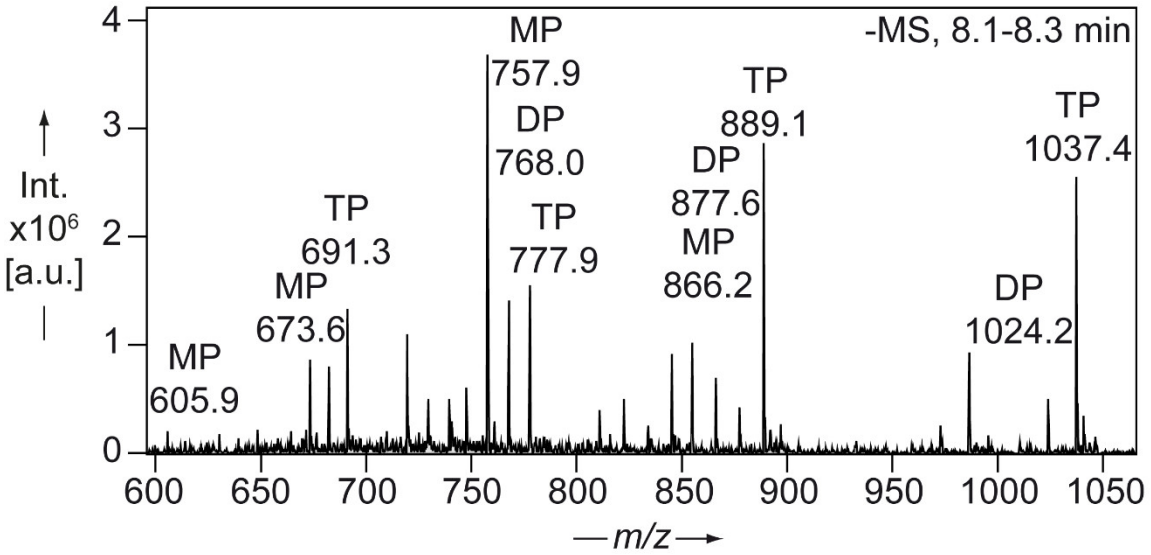

Figure S7. Raw ESI$^-$ traces of spin labeled **RNA^{NO}** with assigned peaks for 5'-mono- (MP), di- (DP) and triphosphate (TP).

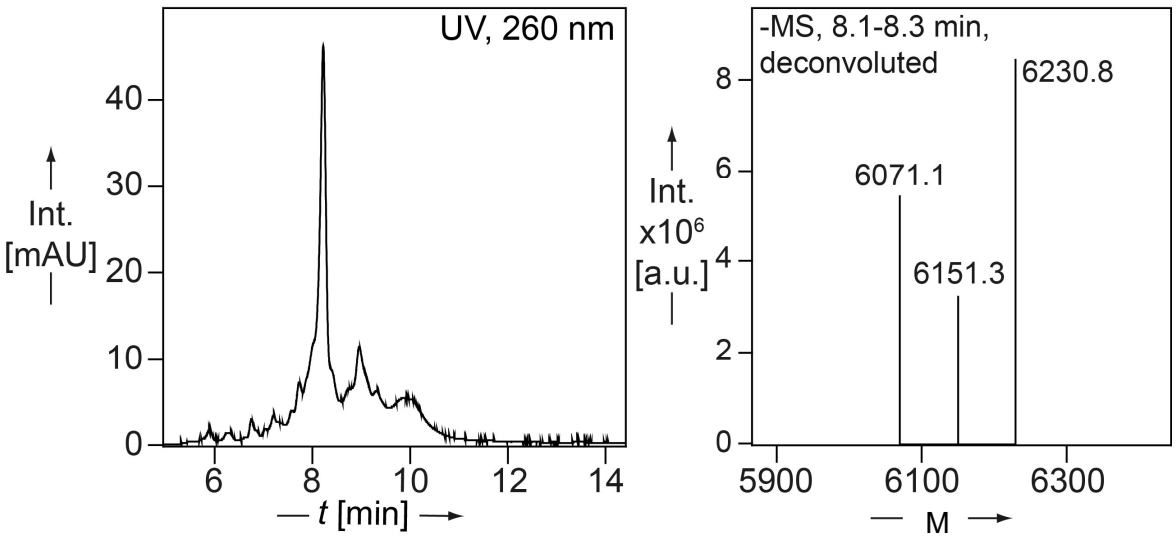

Figure S8. LC-MS analysis showing the UV-trace at 260 nm (left panel) and deconvoluted ESI$^-$ spectrum (right panel) of a crude **RNA^{NO}** transcription ($M_{calcd.}$ for **RNA^{NO}**: 5'-MP = 6070.4, found: *m*/*z* = 6071.1; 5'-DP = 6150.4, found: M = 6151.3; 5'-TP = 6230.4, found: M = 6230.8).

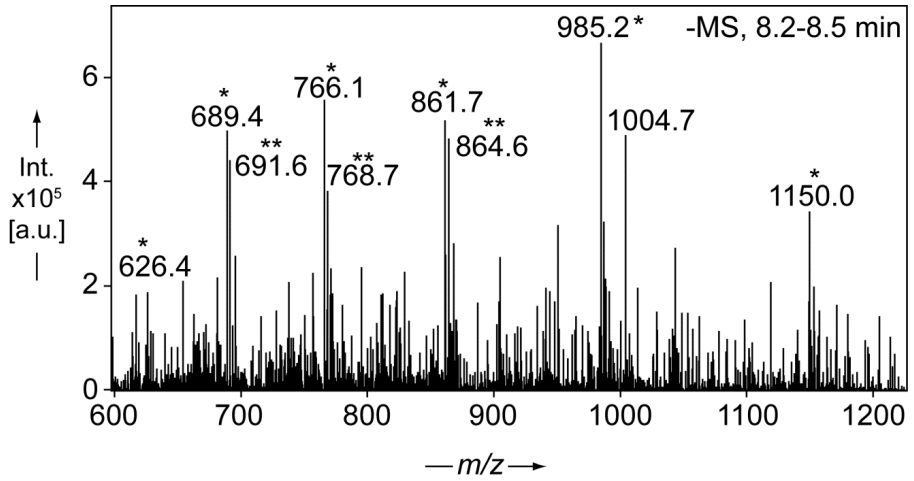

Figure S9. Raw ESI$^-$ traces of spin labeled **RNA_ext^{NO}**; peaks marked by */** are corresponding to 5'-TP+Na$^+$ and 5'-TP+2Na$^+$, respectively.

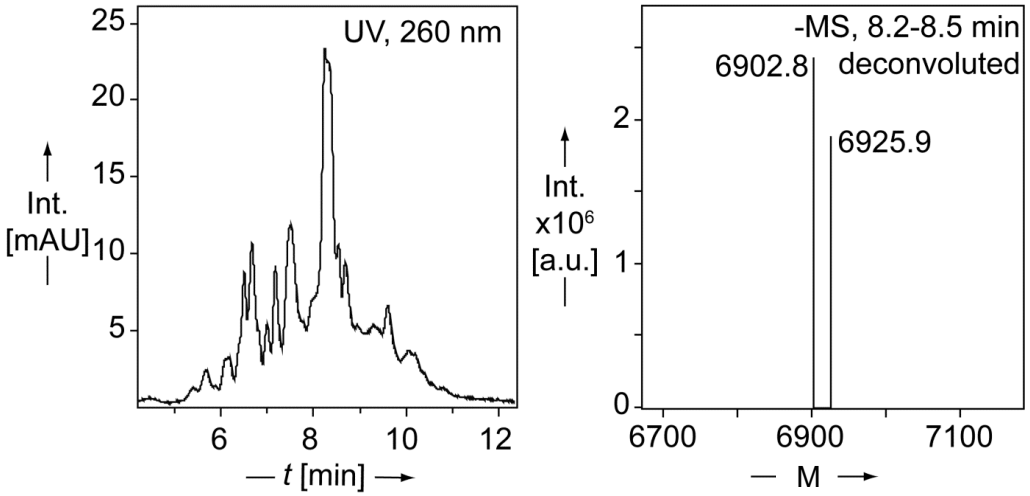

Figure S10. LC-MS analysis showing the UV-trace (left panel) and deconvoluted ESI$^-$ spectrum (right panel) of a crude **RNA_ext^{NO}** transcription ($M_{calcd.}$ for 5'-TP+Na = 6902.8, found: M = 6902.8; $M_{calcd.}$ for 5'-TP+2Na$^+$ = 6925.8, found: M = 6925.9.

*Assessing the incorporation efficiency of **1** by T7 RNA polymerase*

Of four individually prepared crude DNase-digested transcription reactions yielding **RNA^{NO}** (see S13 section *in vitro transcription*) 5 µL samples were taken and analyzed via 20% denat. PAGE (see S12 section *PAGE*) (Figure S11, left panel). The band intensities corresponding to the full-length RNA sequence and the truncated transcript (run-off of the polymerase before/at **TPT3^{NO}** incorporation) were subjected to a software-assisted evaluation (*AIDA*, *Raytest*). For this construct 78.3 ± 2.1% full-length and 21.7 ± 2.1% truncation were observed.

In a similar experiment 71.9 ± 3.2% full-length product and 28.1 ± 3.2% truncated RNA were obtained of six individually prepared transcriptions yielding **RNA_ext^{NO}** (Figure S11, right panel).

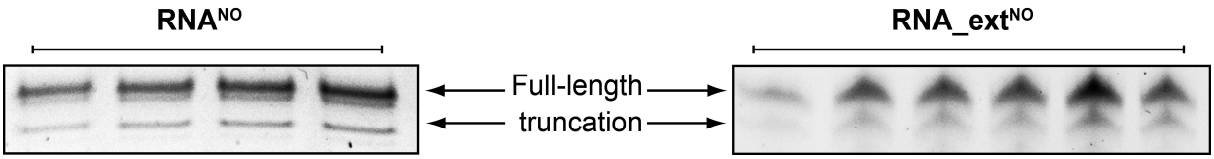

Figure S11. 20% denat. PAGE showing full-length vs. truncated RNA transcripts **RNA^{NO}** and **RNA_ext^{NO}**, respectively.

PAGE images

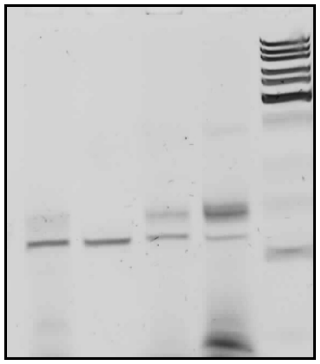

Figure S12. Complete lanes of the 20% denaturing polyacrylamide gel as shown in Figure 2, main text. Marker: *Thermo Scientific GeneRuler* Ultra Low Range DNA Ladder (ULR).

CD Spectroscopy

Oligonucleotides (5 µM) were hybridized in 145 mM NaCl, 10 mM NaH_2PO_4, 10 mM Na_2HPO_4, pH 7.0 by heating to 70 °C for 5 min, followed by a gradient 70 → 18 °C, cooling rate 2 °C min^{-1}. CD experiments were recorded on a *JASCO J-810* spectropolarimeter at 25 °C (0.1 cm high precision cell, *Hellma Analytics*) by averaging 10 scans (220-340 nm, 100 nm min^{-1}, response time = 0.1 s). Buffer spectra were subtracted from the data obtained.

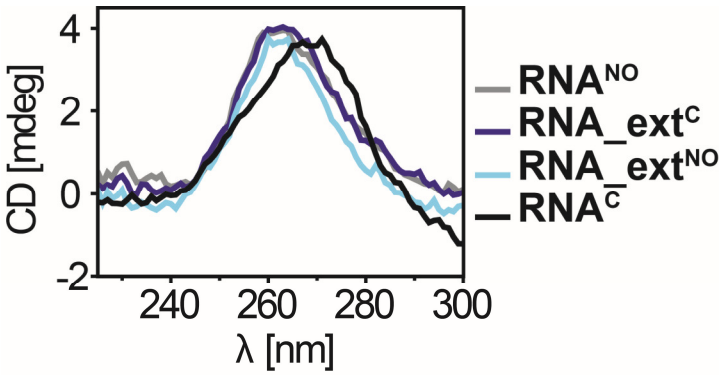

Figure S13. CD spectra of **RNA^{NO}** duplex, **RNA_ext^{NO}** duplex and the corresponding unmodified RNA duplexes **RNA^{C}** and **RNA_ext^{C}**.

UV melting curves

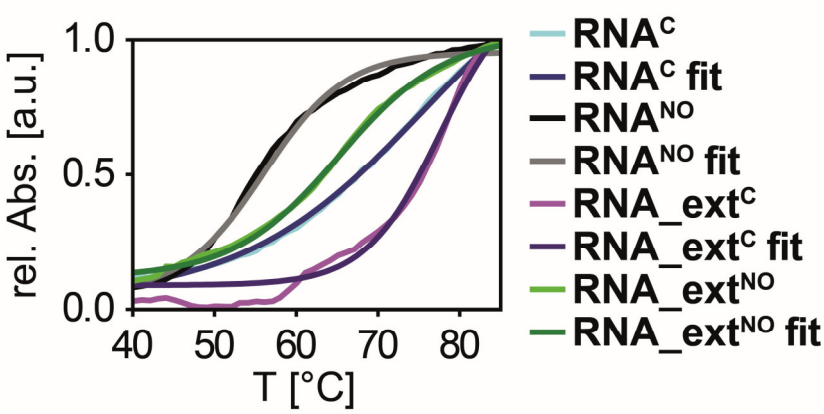

Figure S14. UV melting curves (average of three measurements) of **RNA^{NO}** duplex, **RNA_ext^{NO}** duplex and the corresponding unmodified RNA duplexes **RNA^{C}** and **RNA_ext^{C}** overlaid with fitted data. Thermal denaturation experiments of modified and unmodified oligonucleotides were carried out on a *Cary 100 UV-Vis* spectrophotometer (*Agilent Technologies*). 1 µM samples were prepared in 100 µL phosphate buffer (145 mM NaCl, 10 mM NaH_2PO_4, 10 mM Na_2HPO_4, pH 7.0), annealed 5 min at 70 °C followed by cooling to 18 °C with 2 °C min^{-1} and analyzed in micro-cuvettes (*Hellma Analytics*). The temperature range for melting curve measurements was set from 12 °C to 85 °C with a rate of 1.0 °C min^{-1}.

Melting points were determined from three independent measurements:

Table S1. Melting temperatures of RNA duplexes used in this study.

RNA	T_m
RNA^{NO}	56.0 °C ± 0.2 °C
RNA^{C}	75.8 °C ± 0.8 °C
RNA_ext^{NO}	65.2 °C ± 0.4 °C
RNA_ext^{C}	77.6 °C ± 1.3 °C

Cleavage activity of the spin labeled glmS ribozyme construct

To the EPR sample (prepared as stated below) was added 3.5 µL of a 2 mM ribozyme cofactor glucosamine-6-phosphate (GlcN6P) solution, resulting in a final concentration of ~80 µM. The cleavage reaction was allowed to proceed for 1 h at room temperature.

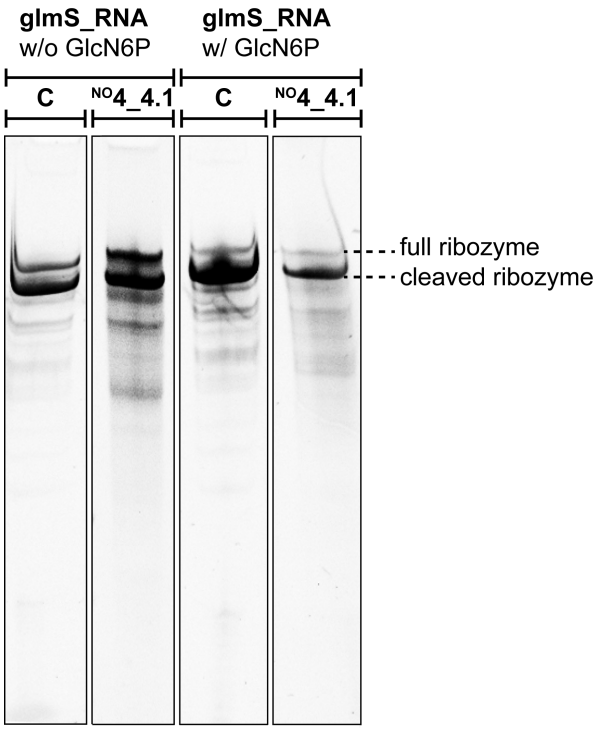

Figure S15. 12% denaturing PAGE analysis of glmS RNA constructs before and after incubation with GlcN6P (final concentration 80 µM).For the unmodified ribozyme and the construct bearing modifications in helix P4 and P4.1 (**glmS^{NO}4_4.1**), complete cleavage of the ribozyme is observed, indicating proper folding of the spin labeled ribozyme.

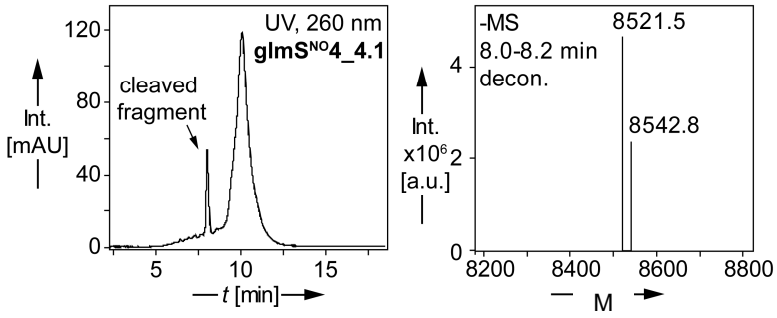

Fig. S16. LC-MS analyses of **glmS^{NO}4_4.1** (80 pmol) after incubation with cofactor GlcN6P. Left panel shows UV trace at 260 nm, right panel shows deconvoluted ESI$^-$ data of the small peak at ~8 min (cleaved fragment, sequence 5'-G GAU UAU UGC UUU ACC UAU AAU UAU A-3'-cP); $M_{calcd.}$ for 5'-TP+Na$^+$ = 8521.9, found: 8521.3 or 8521.5; $M_{calcd.}$ for 5'-TP+2Na$^+$ = 8542.9, found: 8542.2 or 8542.8.

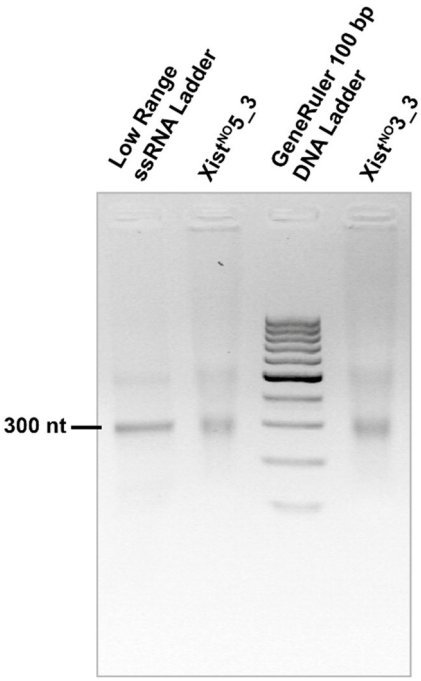

Figure S17. 2 % Agarose gel of purified Xist RNA constructs **Xist^{NO}3_3** and **Xist^{NO}5_3**.

EPR spectroscopy

Sample preparation for EPR measurements

RNA duplexes **RNA^{NO}** and **RNA_ext^{NO}** were dissolved in 80 µL phosphate buffer containing 145 mM NaCl, 10 mM NaH_2PO_4, 10 mM Na_2HPO_4, pH 7.0, and hybridized by heating to 70 °C for 5 min, followed by a gradient 70 → 18 °C with a cooling rate of 2 °C min^{-1}. For PELDOR measurements, RNA solutions were lyophilized after hybridization and then dissolved in sterile filtered D_2O supplemented with 20% deuterated ethylene glycol.

The following RNA amounts were employed for PELDOR experiments (dissolved in 80 µL buffer): **RNA^{NO}**: 1.28 nmol, **RNA_ext^{NO}**: 1.2 nmol.

For construct **glmS^{NO}4_4.1** 750 pmol purified RNA was supplemented with $MgCl_2$ to a final sample concentration of 1 mM and lyophilized. Next, freeze-dried sample was dissolved in 50 µL PELDOR buffer (145 mM NaCl (*Acros Organics*), 10 mM Na_2HPO_4 (*Carl Roth*), 10 mM NaH_2PO_4 (*Carl Roth*), in D_2O (99.9 %, *Deutero)*, sterile filtered) and hybridized as described before. Finally, 12.5 µL ethylene glycol-d_6 (*Sigma-Aldrich*) was added.

Xist^{NO}5_3 and **Xist^{NO}3_3** supernatants after purification applying the NucleoSpin® Gel and PCR Clean-Up Kit (Macherey-Nagel) were taken for concentration and buffer exchange using Amicon® Ultra 3K devices (Merck) according to the manufacturers' protocol, reconstituting the concentrates with 450 µL PELDOR buffer (145 mM NaCl (*Acros Organics*), 10 mM Na_2HPO_4 (*Carl Roth*), 10 mM NaH_2PO_4 (*Carl Roth*), in D_2O (99.9 %, *Deutero)*, sterile filtered) twice. Purified **Xist^{NO}5_3** and **Xist^{NO}3_3** in PELDOR buffer was transferred to a 1.5 mL Eppendorf tube and brought to 50 µL volume adding PELDOR buffer for Xist^{NO}5_3 or

PELDOR buffer and $MgCl_2$ (*Alfa Aesar*, 100 mM, sterile filtered) in D_2O (99.9 %, Deutero) to a final concentration of 1 mM for $Xist^{NO}3\_3$. For hybridisation the RNA was heated to 70 °C for 5 min, then chilled to 18 °C with a 2 °C min^{-1} cooling rate in an Eppendorf Thermomixer®. Following, 12.5 µL ethylene glycol-d_6 (*Sigma-Aldrich*) were added.

EPR measurements

Continuous-wave-(cw)-X-band electron paramagnetic resonance spectroscopy

10 µL samples of the spin-labeled RNA constructs were used to record room temperature *cw*-X-band EPR spectra on an *EMXnano* spectrometer from *Bruker*. The samples were measured at room temperature with a microwave power of 0.32 mW, a modulation amplitude of 1 G, a time constant of 20.48 ms, a conversion time of 20.10 ms.

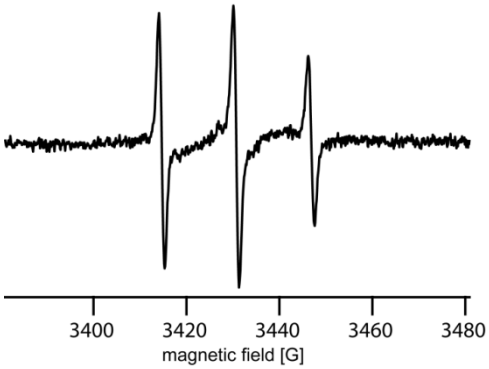

Figure S18. *cw*-EPR spectrum of **RNA^{rNO}** (rigid spin label).

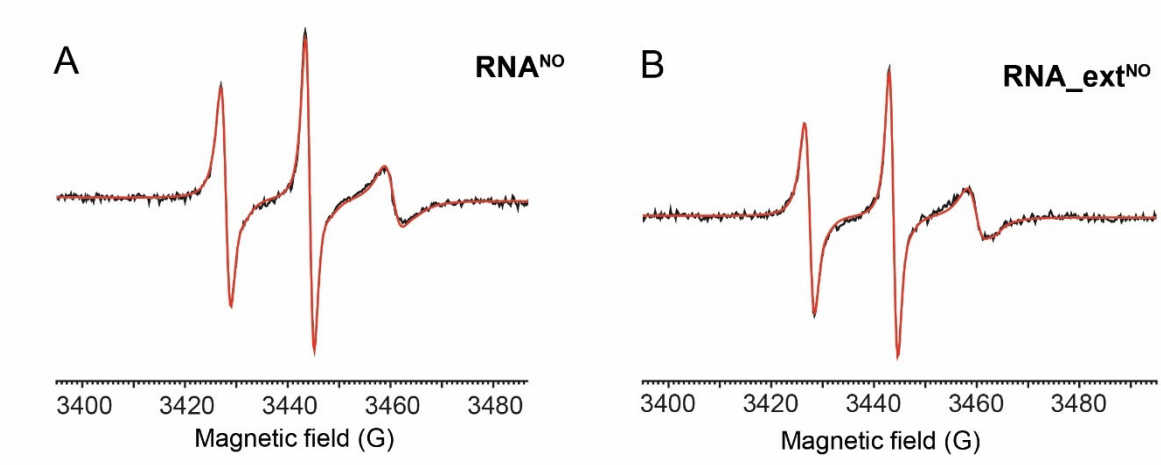

Figure S19. Experimental (black lines) and simulated (red lines) *cw*-EPR spectra of **RNA^{NO}** (A, [spins] = 16.8 µM spins, [A_{260}] = 16.7 µM, 99%), **RNA_ext^{NO}** (B, [spins] = 9.0 µM spins, [A_{260}] = 15.0 µM, 60%)**.** The experimental spectra were simulated using the program *EasySpin* (*http://www.easyspin.org/*).

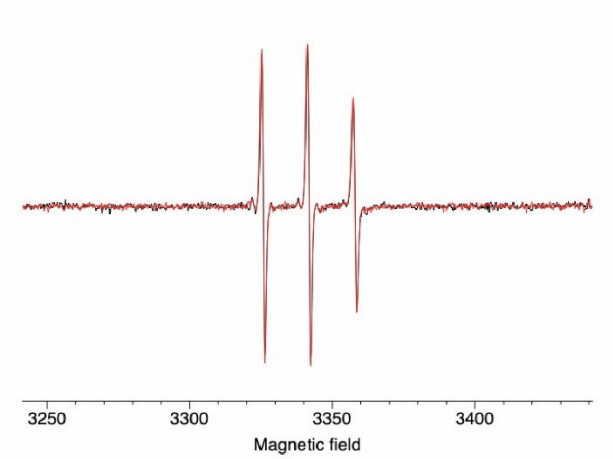

Figure S20. Stability test of spin labeled triphosphate **TPT3^{NO}** TP **1** (Black: t=0, red: t=16h). **TPT3^{NO}** TP was incubated in transcription buffer adding T7 RNA polymerase as described on page S15 at 37°C for 16 h. cw-EPR spectra were measured before and after 16 h incubation.

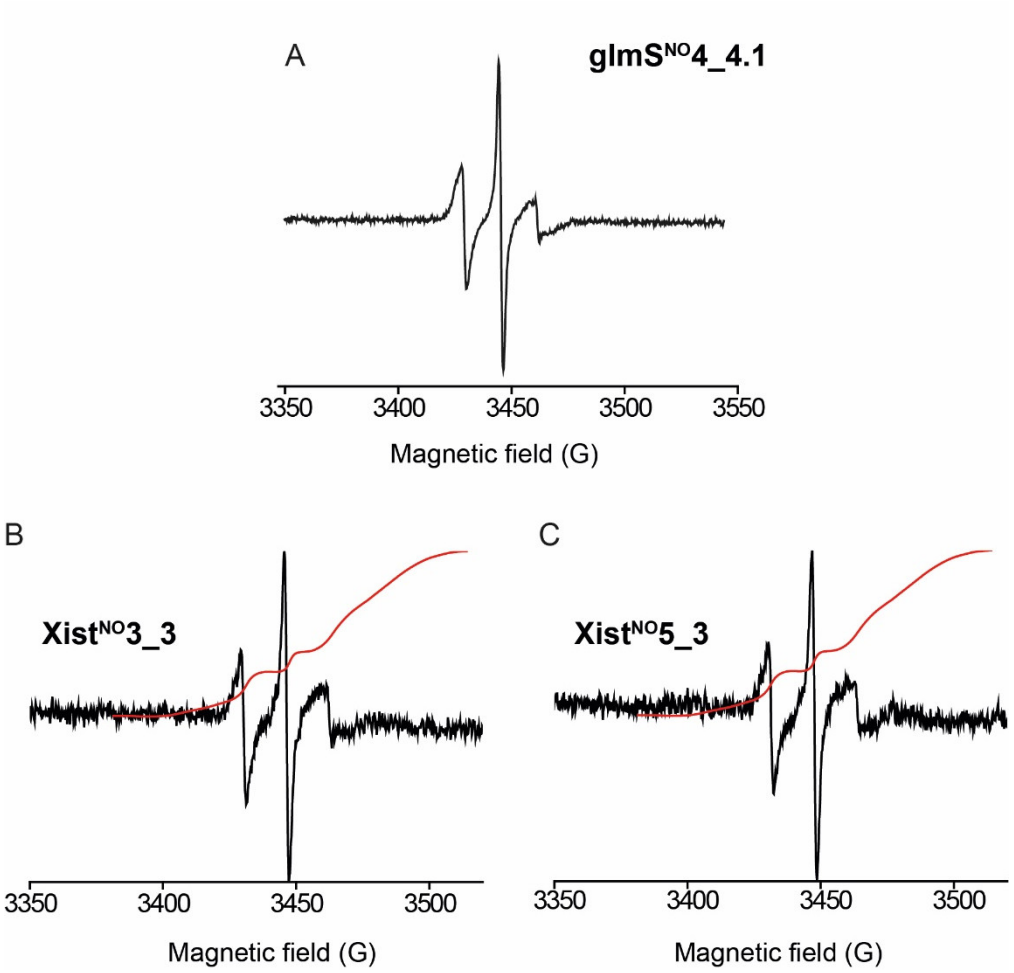

Figure S21. *cw*-EPR spectra of **glmS^{NO}4_4.1** (A, [spins] = 34 µM spins (2 internal labels per RNA), [A_{260}] = 30 µM, 57 %;, **Xist^{NO}3_3** (B, [spins] = 6.6 µM spins (2 internal labels per RNA), [A_{260}] = 7.5 µM, 44 %). and **Xist^{NO}5_3** (C, [spins] = 10.9 µM spins (2 internal labels per RNA), [A_{260}] = 7.2 µM, 76 %).

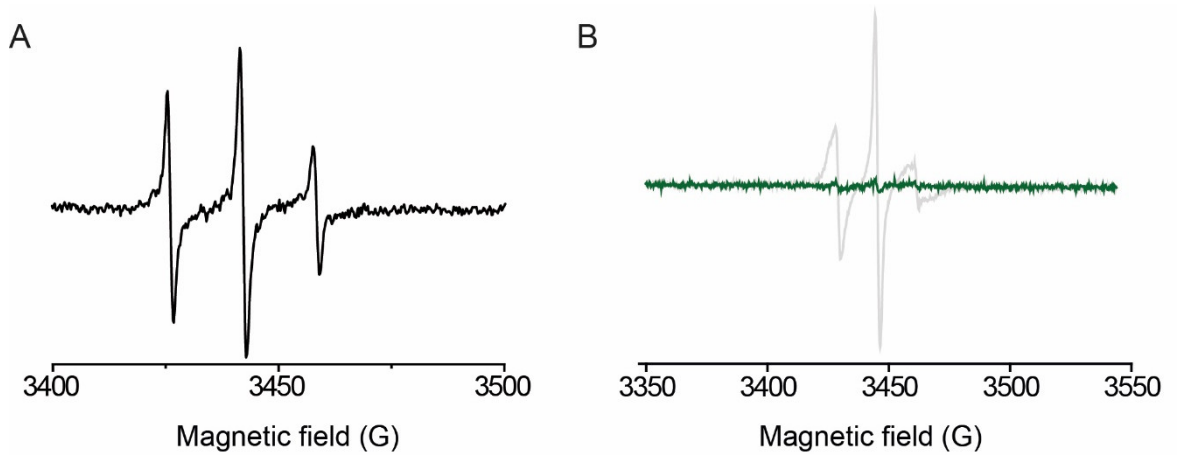

Figure S22. *cw*-EPR spectra of glms ribozyme constructs probing unspecific 3'-extension. A. Transcription from unmodified glmS template prepared using reverse primer **glmS_Pr_RV^{C}** in the presence of **TPT3^{NO}** TP results in extensive unspecific 3'-endlabeling by T7 RNA polymerase; [spins] = 15 µM spins, [A_{260}] = 25 µM, 60 %. B. Transcription from unmodified glmS template prepared using reverse primer **glmS_Pr_RV^{C}_OMe** in the presence of **TPT3^{NO}** TP suppresses unspecific 3'-extension (grey signal, labelled construct shown in Figure S21 A, green signal: control transcription from 2'-OMe modified DNA template containing no unnatural base pairs).

PELDOR spectroscopy

The RNA samples were transferred to a 3 mm quartz Q-band EPR tube and flash-cooled in liquid nitrogen. The PELDOR time traces were recorded on an *ELEXSYS E580* pulsed Q-band EPR spectrometer (*Bruker*), with an *ER 5106QT-2* Q-band resonator. The instrument was equipped with a continuous flow helium cryostat (*CF935*) and temperature control system (*ITC 502*), both from *Oxford Instruments.* The second microwave frequency was coupled into the microwave bridge using a commercially available setup from *Bruker*. All pulses were amplified via a 150 W pulsed traveling wave tube amplifier. PELDOR experiments were performed with the pulse sequence $\pi/2(\nu_A)$-τ1-$\pi(\nu_A)$-(τ1+t)-$\pi(\nu_B)$-(τ2–t)-$\pi(\nu_A)$-τ2-echo. The detection pulses (ν_A) were set to 12 ns for the $\pi/2$ and 24 ns for the π-pulses and applied at a frequency 80 MHz lower than the resonance frequency of the resonator. The pulse amplitudes were chosen to optimize the refocused echo. The $\pi/2$-pulse was phase-cycled to eliminate receiver offsets. The pump pulse (ν_B) was set at the resonance frequency of the resonator and its optimal length (typically 16 ns) was determined using a transient nutation experiment for each sample. The field was adjusted such that the pump pulse was applied to the maximum of the nitroxide spectrum. The pulse amplitude was optimized to maximize the inversion of a Hahn-echo at the pump frequency. All PELDOR

spectra were recorded at 50 K with an experiment repetition time of 1 ms, a video amplifier bandwidth of 20 MHz, and an amplifier gain of 42 dB. The parameter τ1 was set to 260 ns and the maximum of τ2 was set to values ranging from 10 µs. Deuterium modulation was suppressed by addition of 8 spectra of variable τ1 with a Δτ1 of 16 ns. The obtained time traces were divided by a mono exponential decay to eliminate intermolecular contributions and renormalized. Distance distributions were obtained from the background-corrected data by using the program *DEER Analysis 2016* (*http://www.epr.ethz.ch/software.html*) developed by Jeschke *et al.*[8].

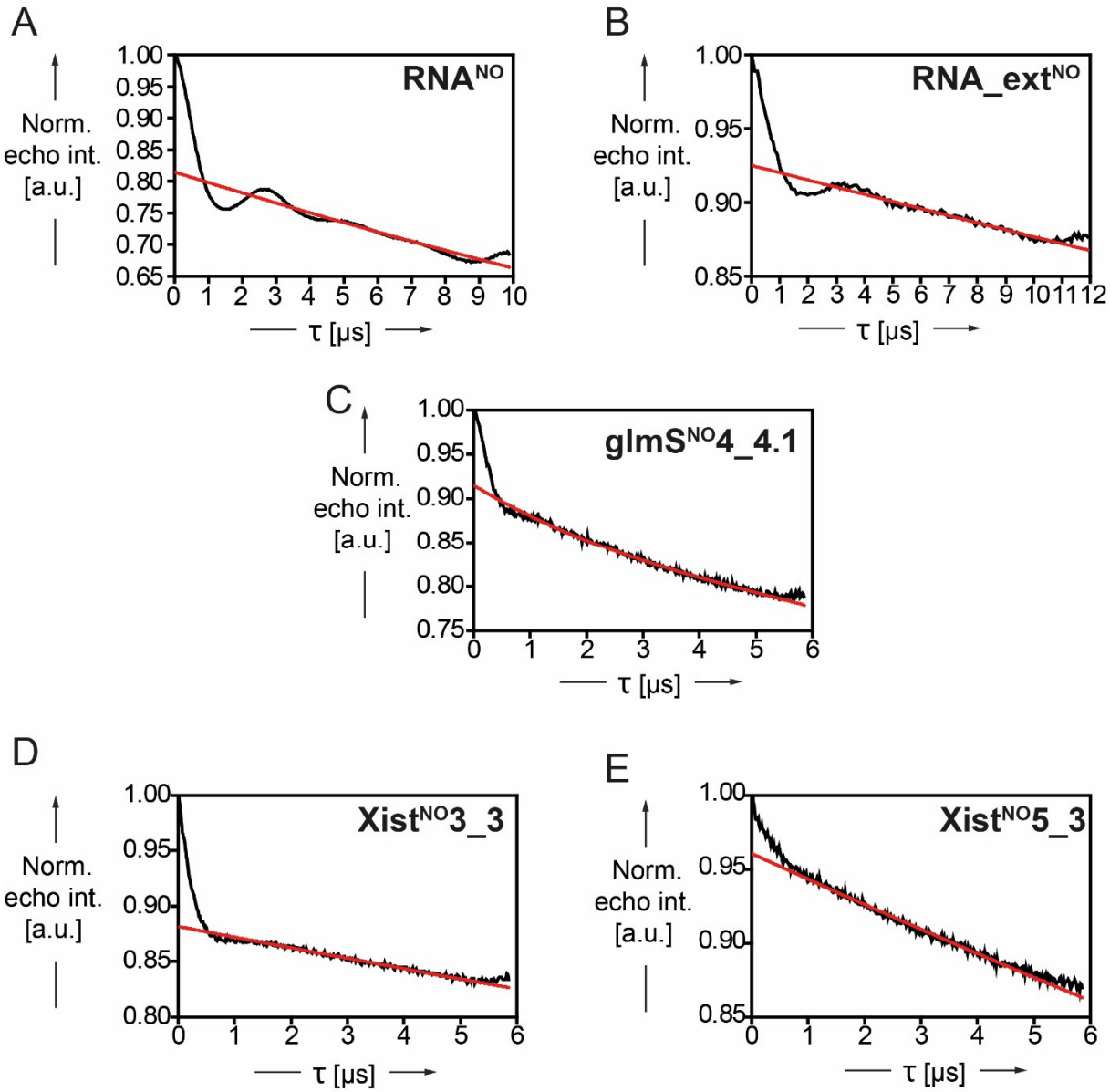

Figure S23. Uncorrected Q-band PELDOR time traces of RNA duplexes **RNA^{NO}** (A), **RNA_ext^{NO}** (B), glmS ribozyme construct **glmS^{NO}4_4.1** (C), **Xist^{NO}3_3** (D) and **Xist^{NO}5_3** (E). The intermolecular background function is shown as red line.

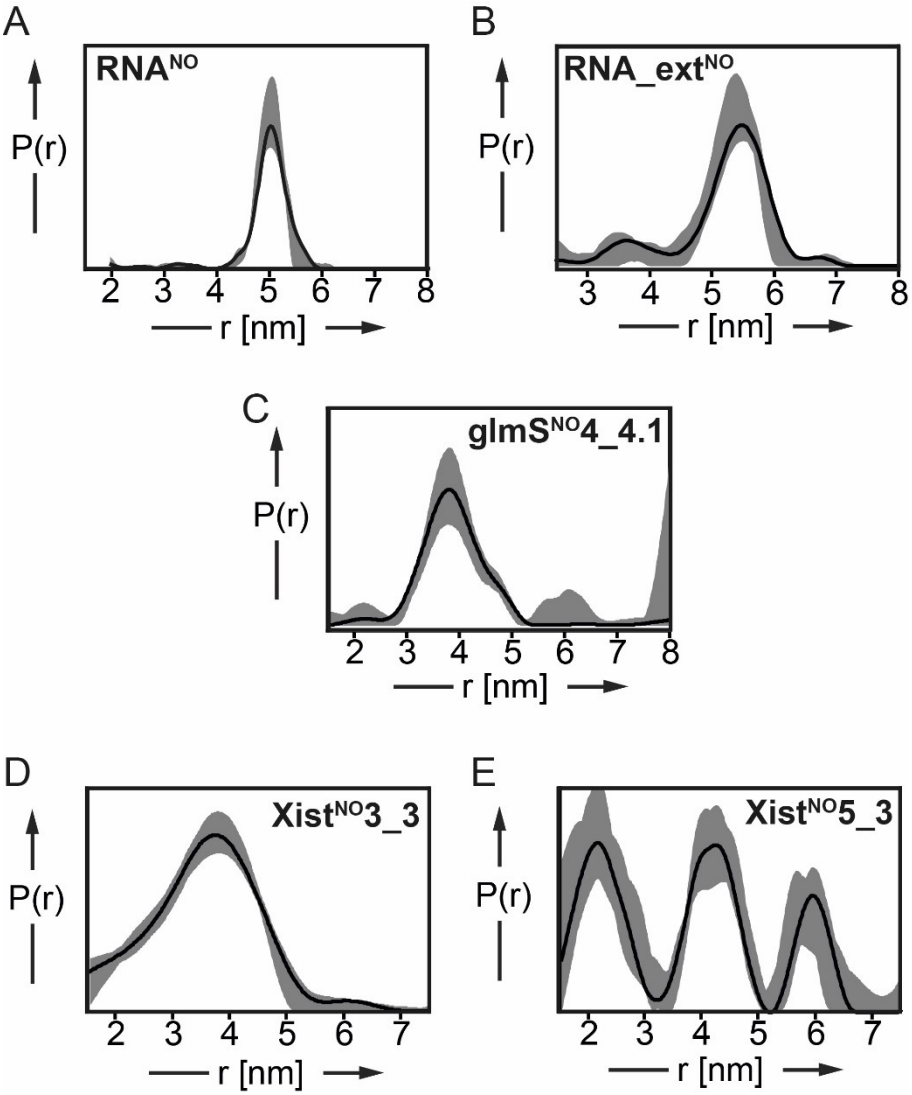

Figure S24. Validation of the PELDOR derived distance distributions shown in Figure 3 and 4. The distance distributions (black curves) are overlaid with a grey area which depicts the uncertainty of the experimentally determined distribution with respect to the background removal procedure. **RNA^{NO}** (A), **RNA_ext^{NO}** (B), glmS ribozyme construct **glmS^{NO}4_4.1** (C), **Xist^{NO}3_3** (D) and **Xist^{NO}5_3** (E).

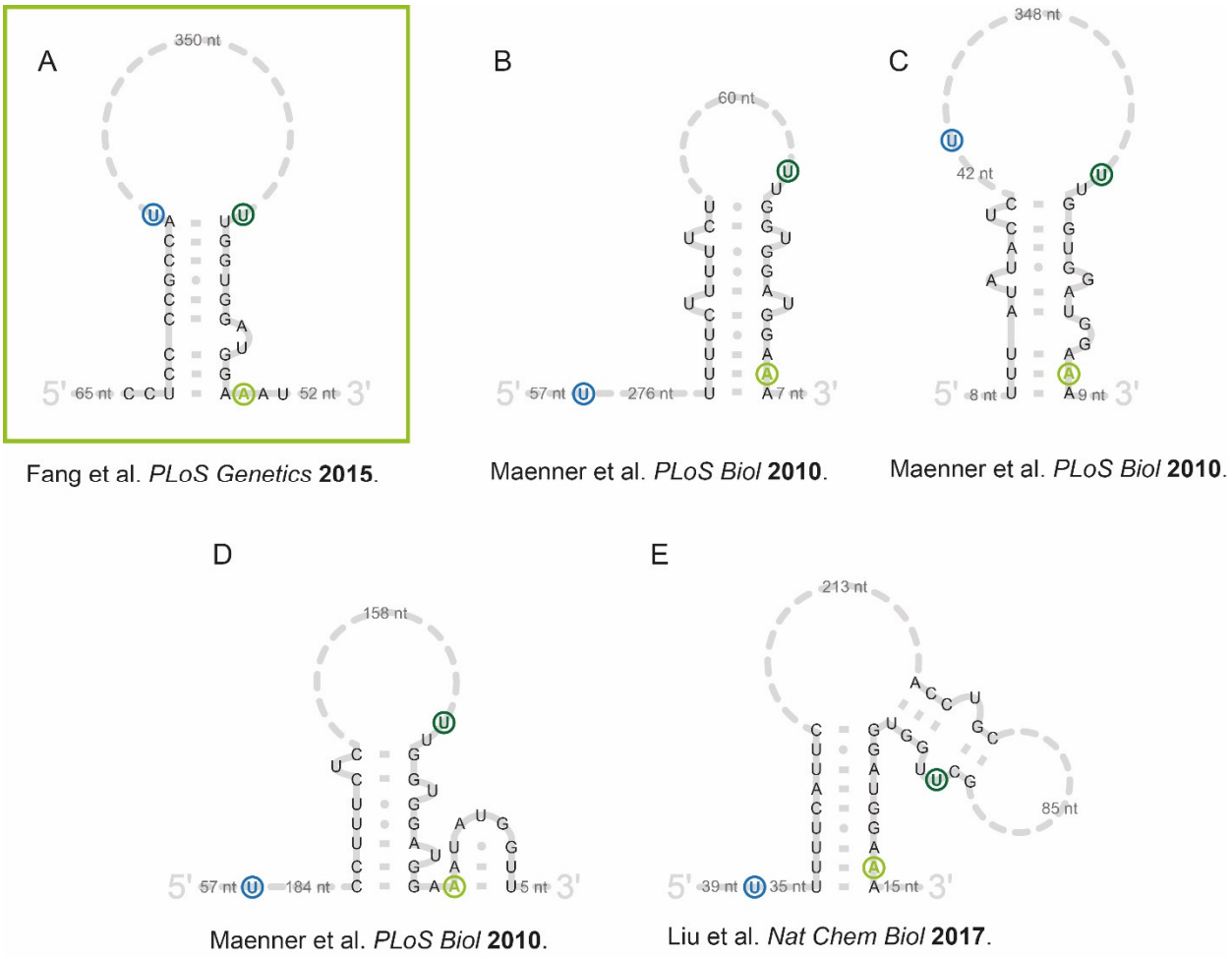

Figure S25. Previously published, proposed theoretical models for the folding of the *M. musculus* Xist A-repeat. Only the 5' and 3' region of the Xist A-repeat RNA is shown for clarity. The positions for introduction of the TPT3^{NO} spin label are marked with circles (blue circles: 5'-modification, dark green: 3'-modification, light green: 3'-modification present in all constructs used in this study).

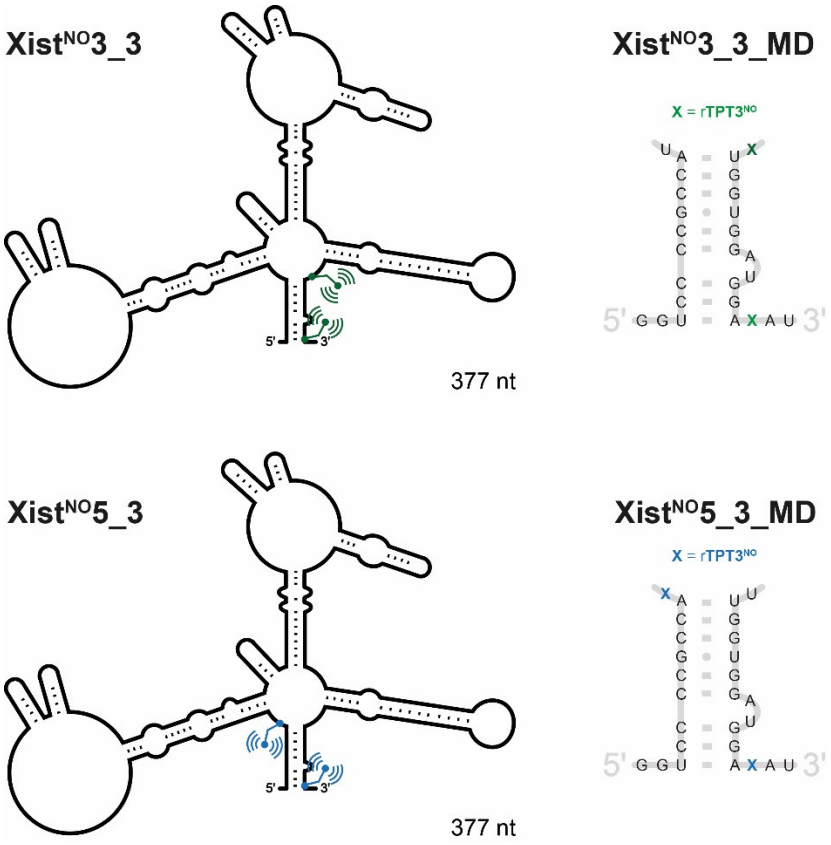

Figure S26. Schematic representation of the duplex structures **Xist^{NO}3_3_MD** and **Xist^{NO}5_3_MD** used for MD simulation mimicking constructs **Xist^{NO}3_3** and **Xist^{NO}5_3**, respectively.

MD Simulation

Parametrization of TPT3^{NO}

The **TPT3^{NO}** residue was parametrized as new residue "**TP**" in CHARMM[9] using Cgenff[10]. 6-31G* ab initio calculations were used on selected groups to adjust the charges, bond lengths, angles and dihedral angles suggested by Cgenff. The used atom definitions and partial charges are listed in Fig, S27 and Tab. S2. The force field parameters corresponding to the atom connections within new "**TP**" residue are deposited in the CHARMM-36-Gromacs[11] parameter file "ffbonded.itp". These data were already published in Domnick et. al.[12] describing the analogue TPC3 residue which contains an additional cyclopropene–tetrazine click unit.

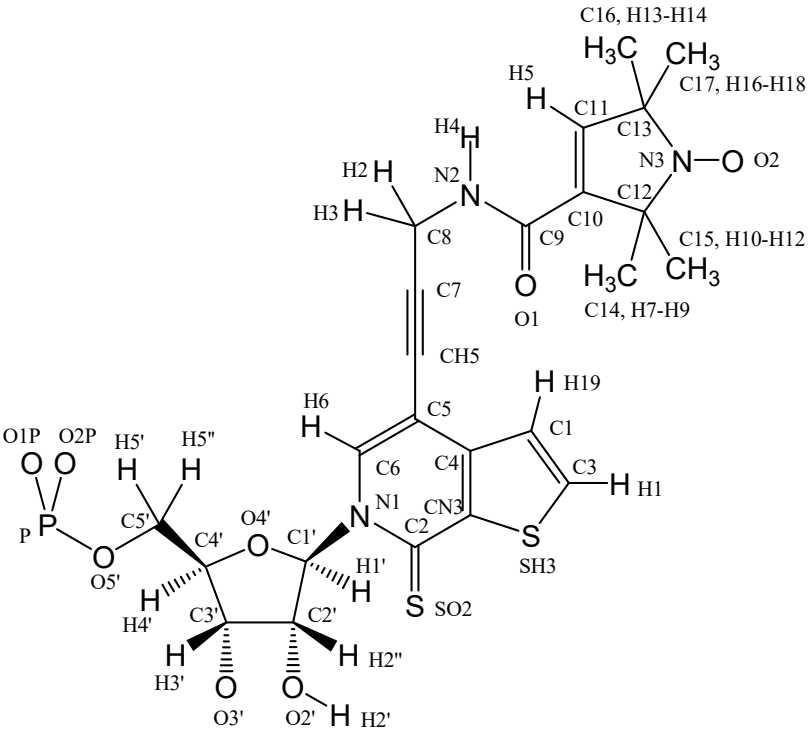

Figure S27. Structure of the spin labeled residue **TPT3^{NO}** with atom definitions. The residue is named **TP** in the used modified Gromacs – Charmm36 force field, see Table S2.

Table S2. Residue topology entry "TP" (spin labeled **TPT3^{NO}** nucleoside) in "merged.rtp" of the Gromacs – Charmm 36 force field**.** The partial charges were suggested by CGenFF[10] (interface 1.0.0, force field 3.0.1) and adjusted using AM1 and 6-31G* QM calculations. The atom definitions are given in Fig. S27.

```
[ TP ]
  [ atoms ]
;  atom   atomtype  charge
   P         P      1.500  0
   O1P       ON3   -0.780  1
   O2P       ON3   -0.780  2
   O5'       ON2   -0.570  3
   C5'      CN8B   -0.080  4
   H5'       HN8    0.090  5
  H5''       HN8    0.090  6
   C4'       CN7    0.160  7
   H4'       HN7    0.090  8
   O4'      ON6B   -0.500  9
   C1'      CN7B    0.160 10
   H1'       HN7    0.090 11
   N1       NN2B   -0.300 12
   C6     CG2R61    0.025 13
   H6      HGR62    0.190 14
   C5     CG2R61    0.105 15
  CH5      CG1T1   -0.005 16
   C4     CG2RC0   -0.095 17
  CN3     CG2RC0    0.060 18
  SH3     SG2R50   -0.050 19
   C2     CG2R63    0.130 20
  SO2      SG2D1   -0.206 21
  C2'       CN7B    0.140 22
 H2''       HN7    0.090 23
  O2'       ON5   -0.660 24
  H2'       HN5    0.430 25
  C3'       CN7    0.010 26
  H3'       HN7    0.090 27
  O3'       ON2   -0.570 28
   C1     CG2R51   -0.250 29
```

```
 C3    CG2R51   -0.069 30
 C7     CG1T1   -0.11  31
 C8     CG321   -0.02  32
 N2     NG2S1   -0.43  33
 C9     CG2O1    0.55  34
C10    CG2R51   -0.10  35
C11    CG2R51   -0.08  36
C12    CG3C50    0.20  37
 N3    NG3C51   -0.09  38
C13    CG3C50    0.20  39
C14     CG331   -0.24  40
C15     CG331   -0.24  41
C16     CG331   -0.24  42
C17     CG331   -0.24  43
 O1     OG2D1   -0.45  44
 H1     HGR52    0.185 45
 H2      HGA2    0.09  46
 H3      HGA2    0.09  47
 H4      HGP1    0.311 48
 H5     HGR51    0.15  49
 O2     OG312   -0.36  50
 H7      HGA3    0.09  51
 H8      HGA3    0.09  52
 H9      HGA3    0.09  53
H10      HGA3    0.09  54
H11      HGA3    0.09  55
H12      HGA3    0.09  56
H13      HGA3    0.09  57
H14      HGA3    0.09  58
H15      HGA3    0.09  59
H16      HGA3    0.09  60
H17      HGA3    0.09  61
H18      HGA3    0.09  62
H19     HGR51    0.209 63

[ bonds ]
   P   O1P
   P   O2P
   P   O5'
 O5'   C5'
 C5'   C4'
 C4'   O4'
 C4'   C3'
 O4'   C1'
 C1'    N1
 C1'   C2'
  N1    C2
  N1    C6
  C2   CN3
  C2   SO2
 CN3   SH3
 CN3    C4
  C4    C5
  C2'   C3'
 C3'   O3'
 O3'    +P
 C2'   O2'
 O2'   H2'
 C1'   H1'
 C2'  H2''
 C3'   H3'
 C4'   H4'
 C5'   H5'
 C5'  H5''
  C5   CH5
  C5    C6
  C6    H6
  C4    C1
  C1    C3
  C1   H19
  C3    H1
  C3   SH3
 CH5    C7
  C7    C8
  C8    N2
  C8    H2
  C8    H3
  N2    H4
```

```
   N2    C9
   C9    O1
   C9   C10
   C10  C11
   C10  C12
   C11  C13
   C11   H5
   C12   N3
   C13   N3
    N3   O2
   C12  C14
   C12  C15
   C13  C16
   C13  C17
   C14   H7
   C14   H8
   C14   H9
   C15  H10
   C15  H11
   C15  H12
   C16  H13
   C16  H14
   C16  H15
   C17  H16
   C17  H17
   C17  H18

[ impropers ]
    C2   CN3    N1   SO2
    C9   C10    N2    O1
```

Preparation of the starting models

The self-complementary RNA duplexes **RNA^{NO}** and **RNA_ext^{NO}** as well as the duplexes mimicking the Xist stem structures **Xist^{NO}3_3_MD** and **Xist^{NO}5_3_MD** (Figure S26) were constructed based on A-form RNA in HyperChem (Release 7.01, *Hypercube, Inc*.) with one **TPT3^{NO}** residue per oligonucleotide (zero and two **TPT3^{NO}** in case of **Xist^{NO}5_3_MD)**. To build the starting structure of the glmS ribozyme construct **glmS^{NO}4_4.1**, the *B. anthracis* glmS crystal structure (PDB code: 3L3C) was converted to the *B. subtilis* sequence in HyperChem. Chains G and R of the PDB structure 3L3C were used. Four Mg^{2+} Ions and eleven water molecules, which are resolved in the X-ray structure of *B. anthracis*, were also included in the starting geometry of *B. subtilis*. The Glc6P in the structure 3L3C of *B. anthracis* was omitted. The conversion of the nucleic acid residues is given in detail in Fig. S.28. All starting structures were placed in cubic boxes, solvated with TIP3P water molecules and Na^+ counterions:

RNA^{NO}: 7.268 nm^3 cubic box, 11950 TIP3P water molecules and 34 Na^+ counterions

RNA_ext^{NO}: 7.3380 nm^3 cubic box, 12250 TIP3P water molecules and 38 Na^+ counterions

glmS^{NO}4_4.1: 14.184 nm^3 cubic box, 91227 TIP3P water molecules and 176 Na^+ counterions

Xist^{NO}5_3: 6.739 nm^3 cubic box, 9666 TIP3P water molecules and 25 Na^+ counterions

Xist^{NO}3_3: 6.353 nm^3 cubic box, 7987 TIP3P water molecules and 25 Na^+ counterions

Md simulations producing inter NO—NO distance distributions

The starting model systems were energy minimized switching alternatively between runs using steepest descent gradients or Polak-Ribiere conjugate gradients until convergence to machine precision. Subsequently, 480ps MD calculations at constant temperature (300 K, NVT) followed by 480 ps MD calculations at constant pressure (1 bar, NPT) equilibrate solvent and ions. Finally, MD trajectories were calculated without restraints or constraints (except bond lengths) or with restraints on H-bonds (see description below for details to individual experiments) at 300 K.

RNA^{NO}:

1000 ns restraints on all base pairs, followed by 1000 ns restraints on only the central two UA pairs (U9-A28 and A10-U27), then followed by 2000 ns simulation without any restraints.

RNA_ext^{NO}:

12 ns restraints on all base pairs, followed by 2000ns without any restraints.

glmS^{NO}4_4.1:

1000 ns restraints on all base pairs, followed by 1000 ns without restraints.

Xist^{NO}3_3

50 ns restraints on all base pairs, followed by 1000 ns without restraints.

Xist^{NO}5_3:

1000 ns restraints on all base pairs.

The resulting time dependent inter-nitroxide distances are listed in Fig. S 29.

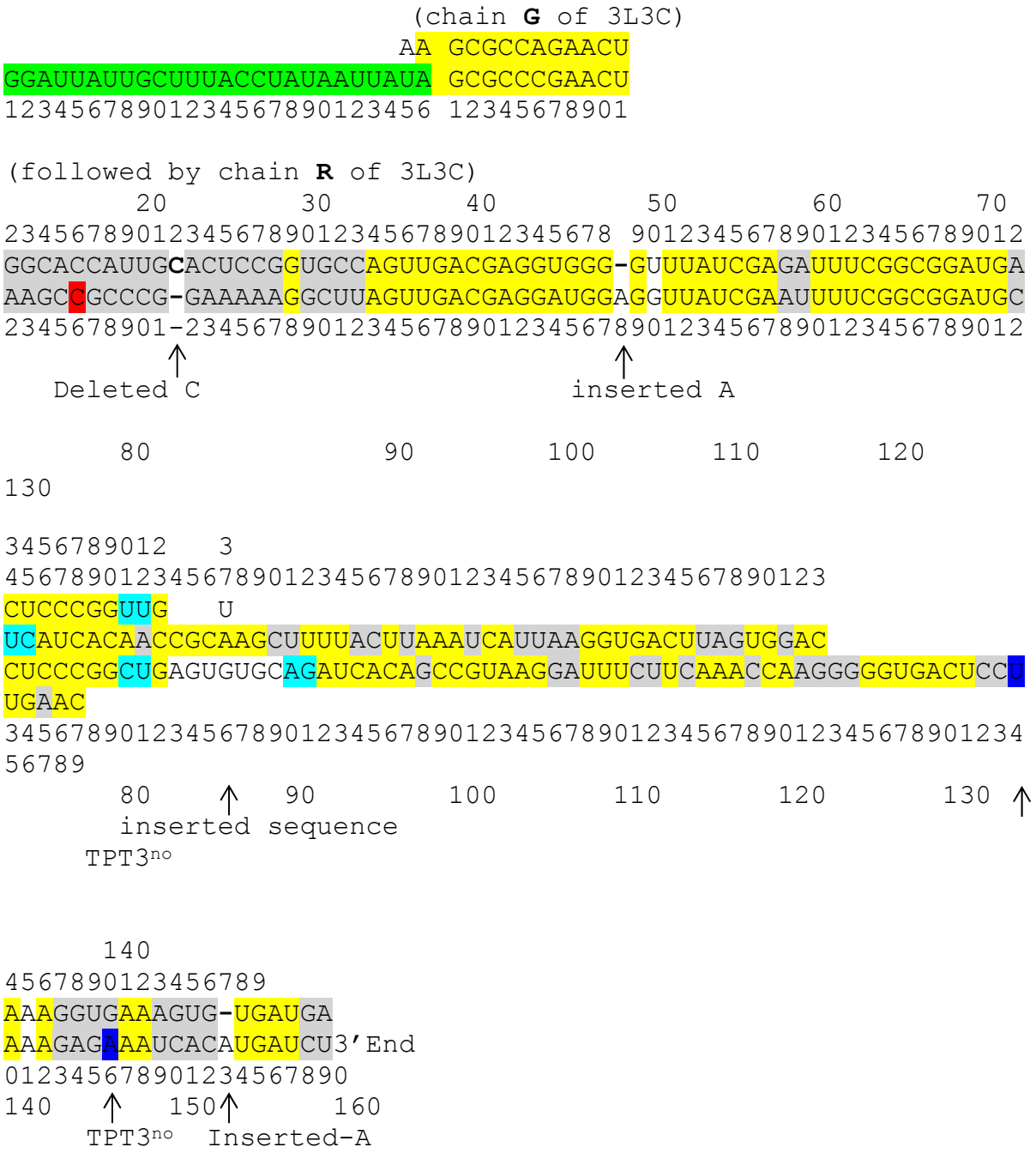

Figure S28. Correlation between the crystal structure sequence of the glms ribozyme in *B. anthracis* (pdb-entry 3L3C) and the starting geometry and sequence of the glms ribozyme in *B. subtilis* used experimentally and in the MD calculations. The upper row contains the *B. anthracis* sequence, the lower row represents the *B. subtilis* sequence.

Further explanations: Yellow marks - Nucleotides are conserved in both sequences: The coordinates in the *B. anthracis* structure were used as starting geometry for the coordinates of the glms *B. subtilis* residues. Grey marks - Nucleotides are different in both sequences: The residues of the *B. anthracis* structure were transformed to glms *B. subtilis* residues using

the coordinates of the ribose units and mutating the nucleobase. Green marks - Additional nucleotides at the 5' terminus of the *B. subtilis* sequence: A chain of 26 nucleotides in helical RNA conformation is added at the 5'- end of the *B. anthracis* sequence building the 5' chain in the *B. subtilis* sequence. Red mark - This C-residue does not exist in the *B. subtilis* sequence, but is used in the experimental constructs **glmS^{NO}4_4.1** and **glmS_RNA^{C}**. It is assumed that the stem P1 will be stabilized by an additional C-G base pair. Blue marks - Positions of TPT3^{NO} residues in **glmS^{NO}4_4.1**.

.

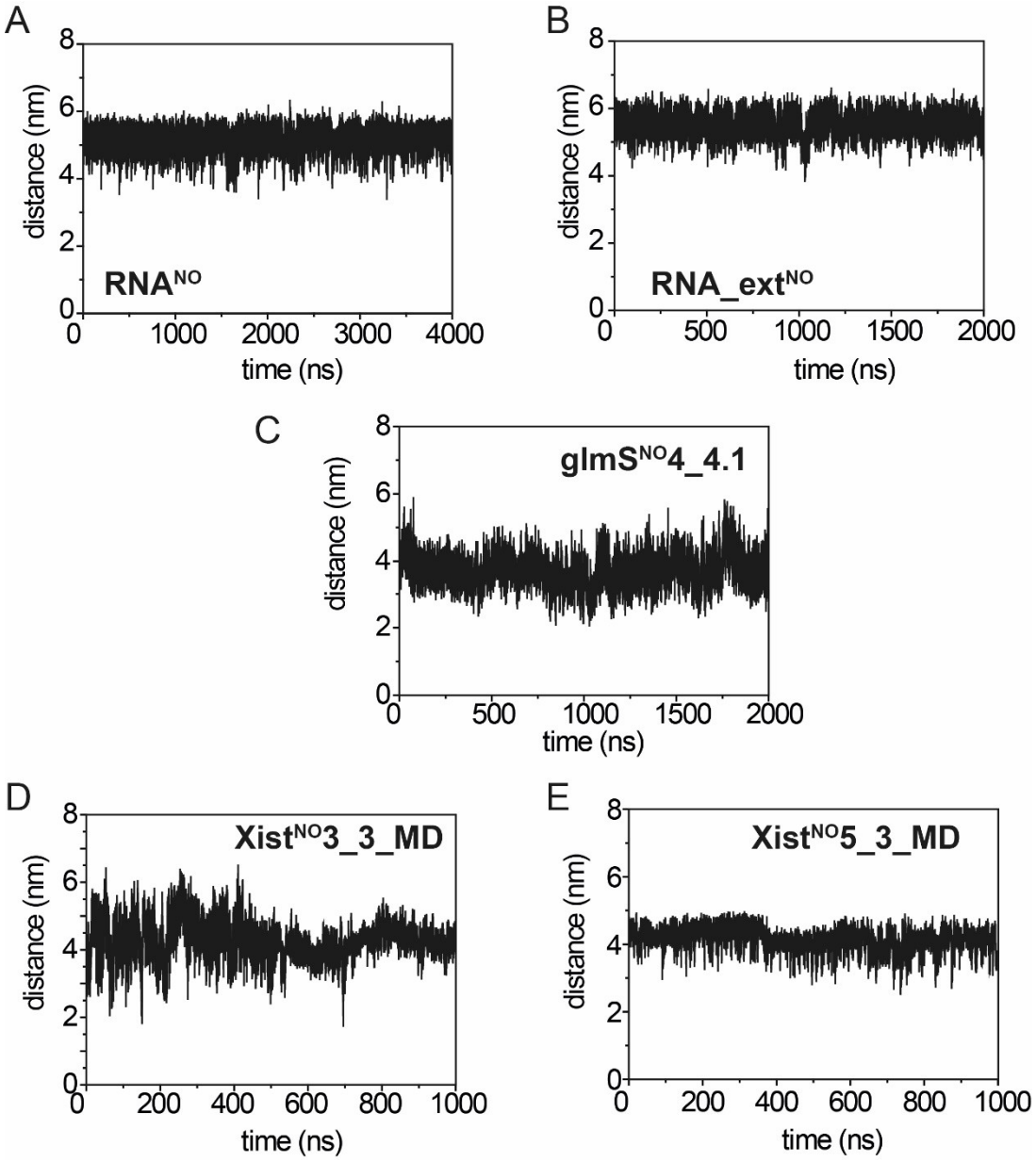

Figure S29. Time dependent evolution of the inter-nitroxide distances in **RNA^{NO}** (A), **RNA_ext^{NO}** (B), glmS ribozyme construct **glmS^{NO}4_4.1** (C), **Xist^{NO}3_3_MD** (D) and **Xist^{NO}5_3_MD** (E).

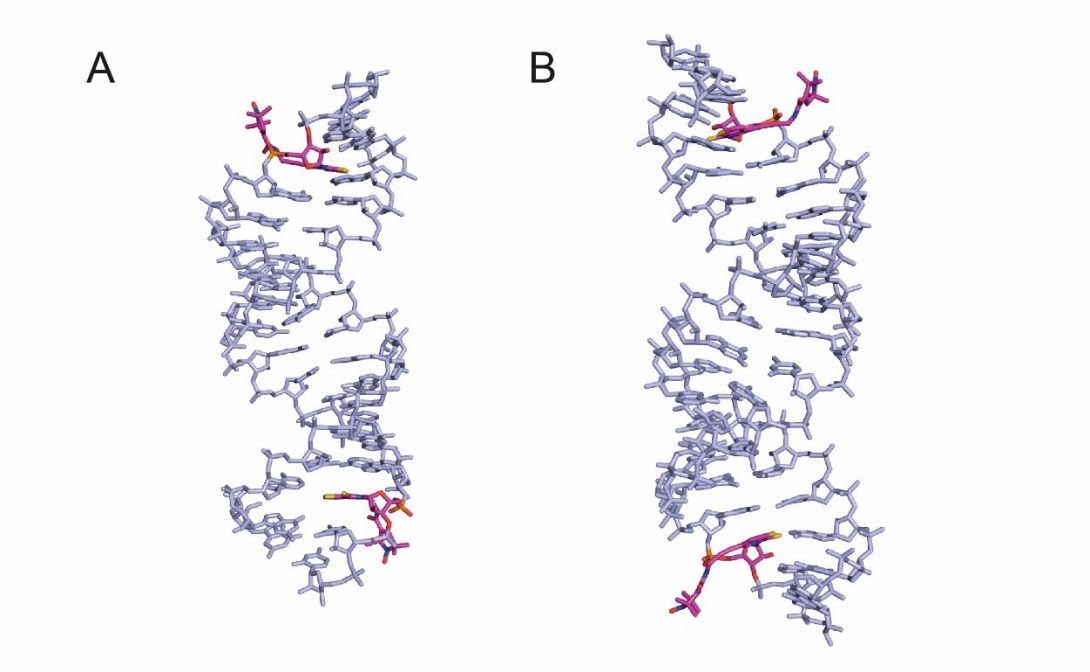

Figure S30. Representative snapshots (MD cluster analysis) of the duplexes **RNA^{NO}** (A), **RNA_ext^{NO}** (B). The **TPT^{NO}** residues are colored in pink.

Spectra

NMR spectra

^{1}H-NMR spectrum of compound **5** ($CDCl_3$, 400 MHz, r.t.).

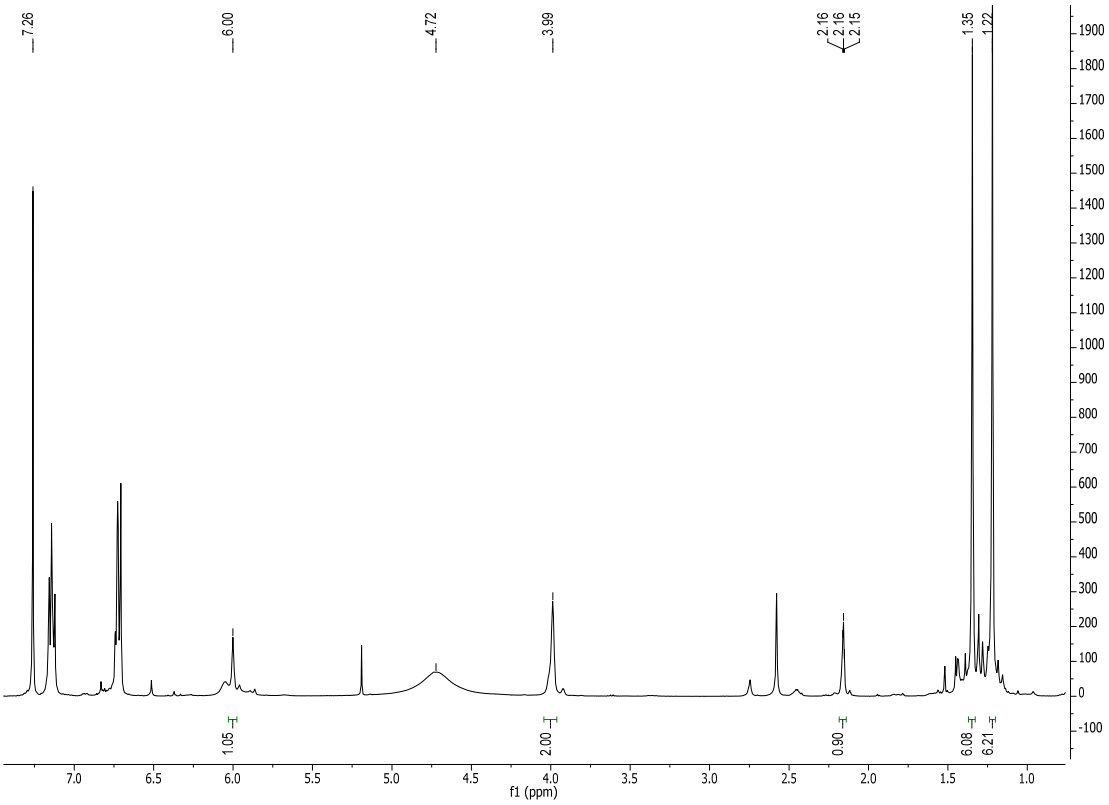

^{13}C-NMR spectrum of compound **5** ($CDCl_3$, 101 MHz, r.t.).

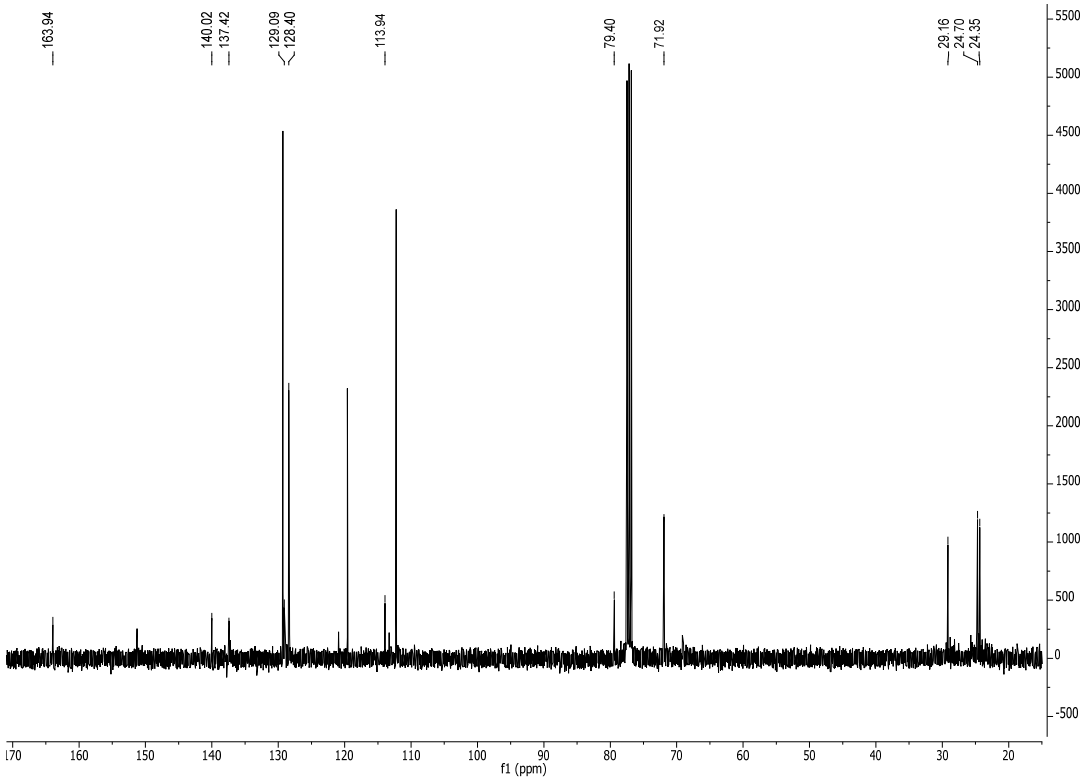

HMQC spectrum of compound **5** ($CDCl_3$, r.t.).

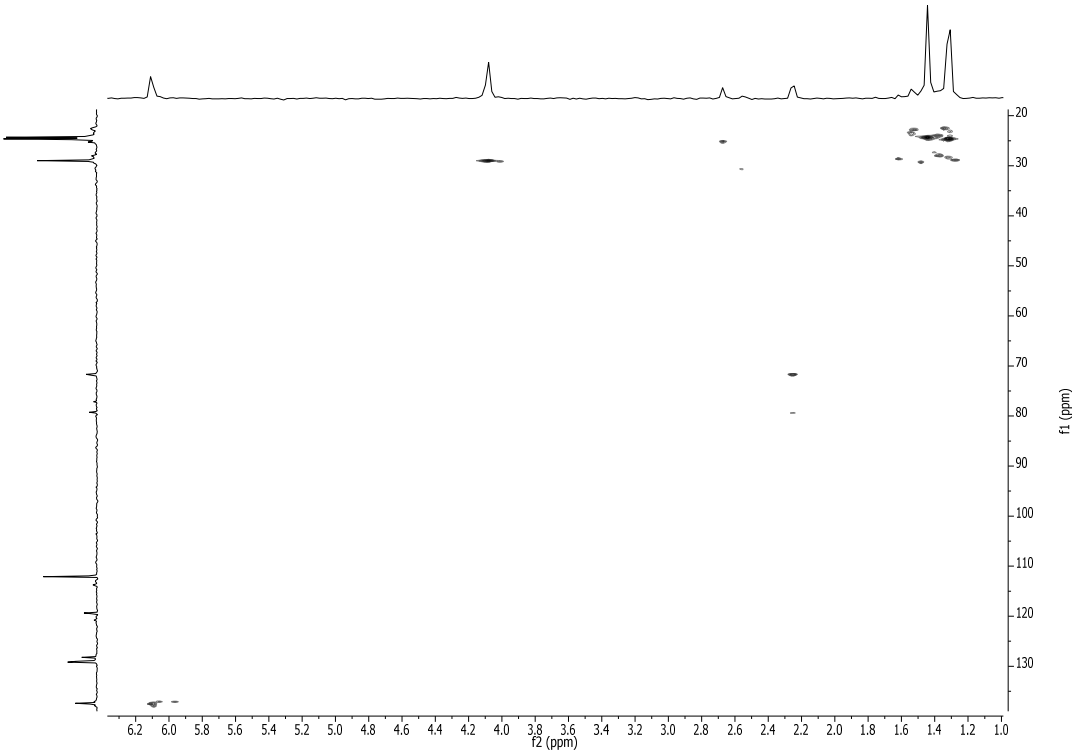

^{1}H-NMR spectrum of compound **6** (CD_3OD, 400 MHz, r.t.).

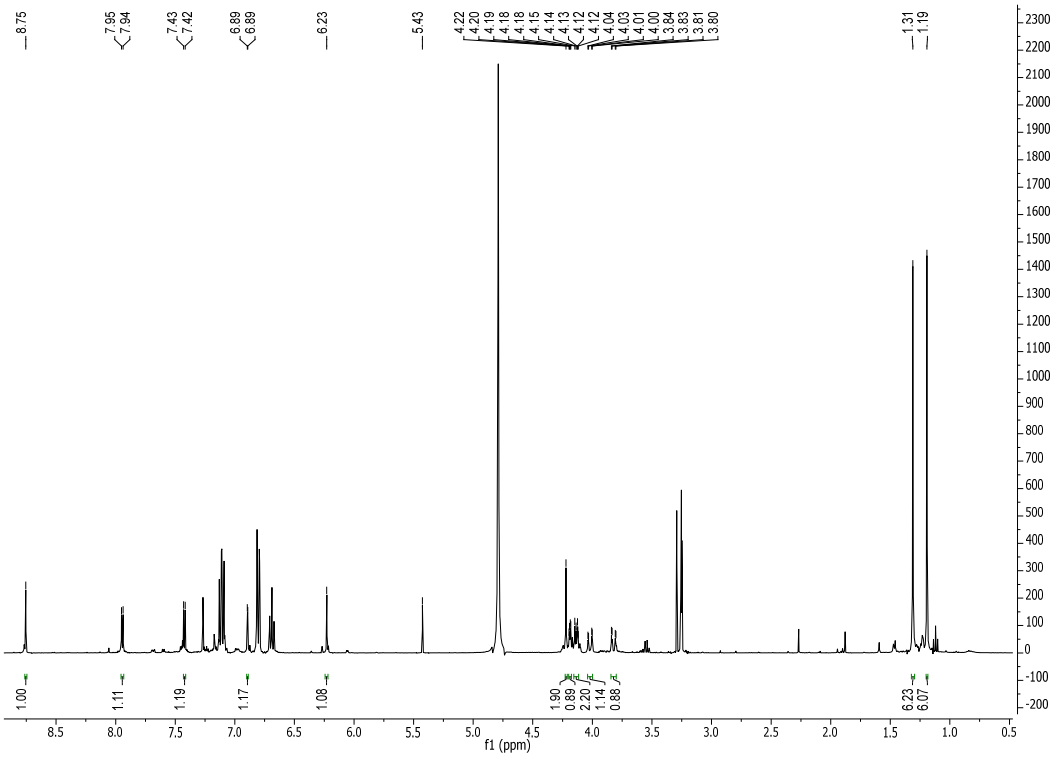

^{13}C-NMR spectrum of compound **6** (CD_3OD, 101 MHz, r.t.).

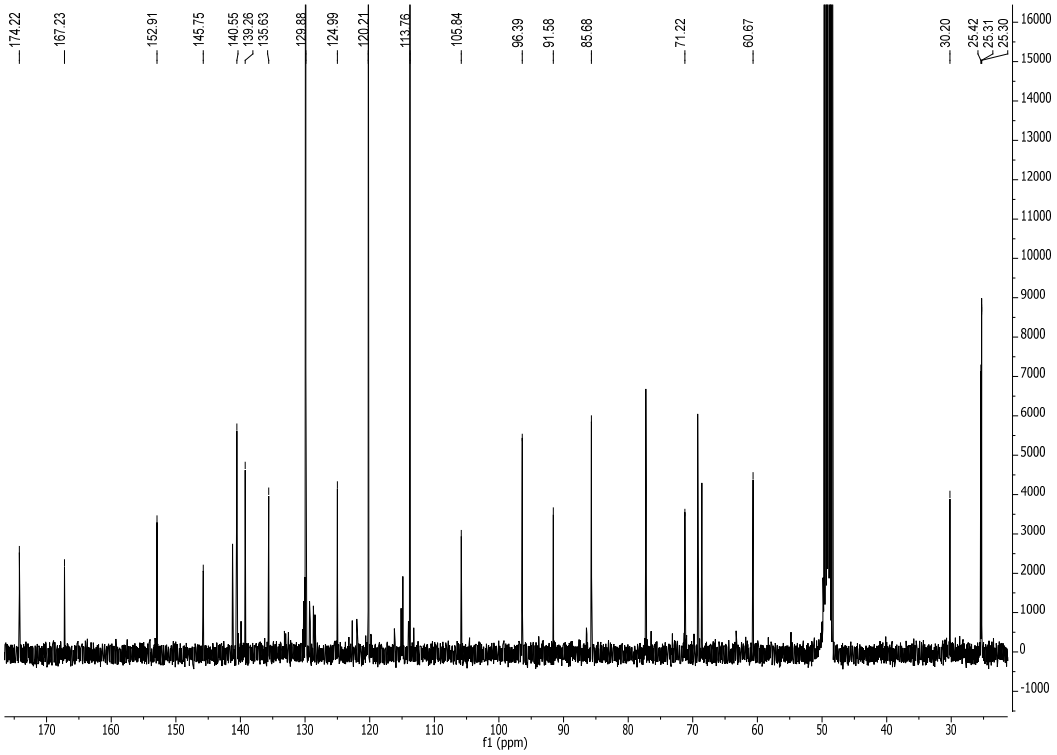

^{31}P-NMR spectrum of compound **1** (D_2O, 162 MHz, r.t.)

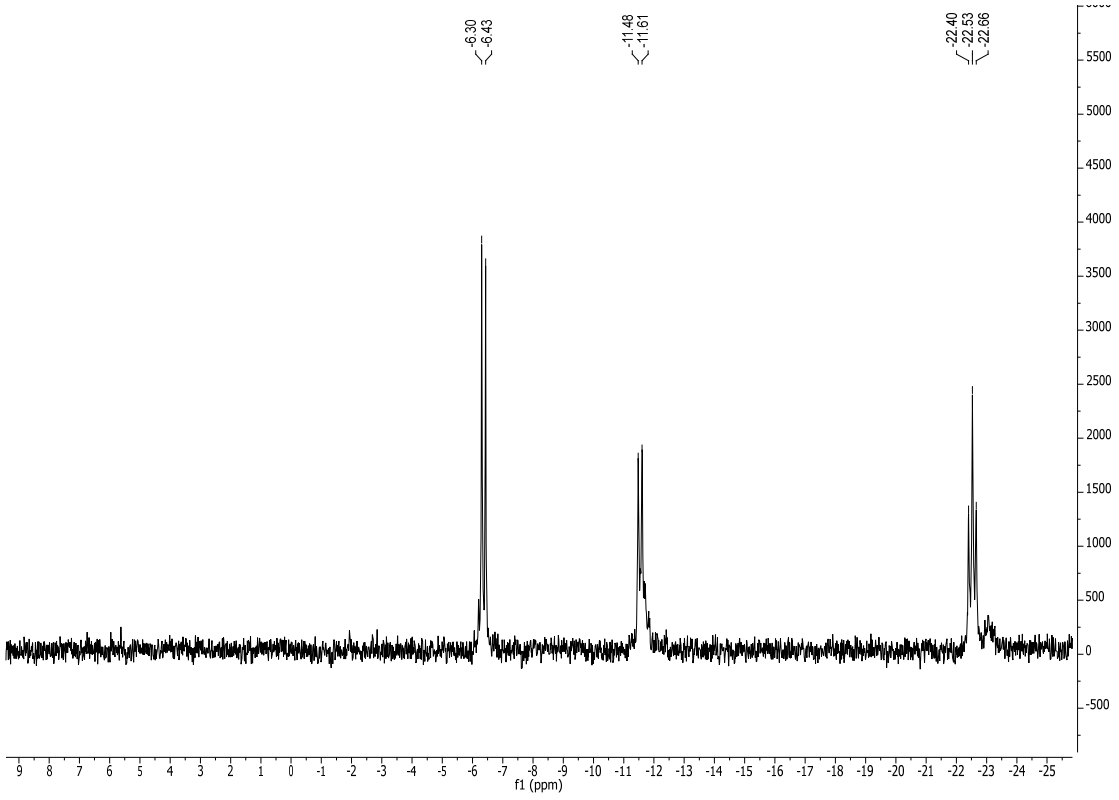

^{1}H-NMR spectrum of compound **8** ($CDCl_3$, 400 MHz, r. t.).

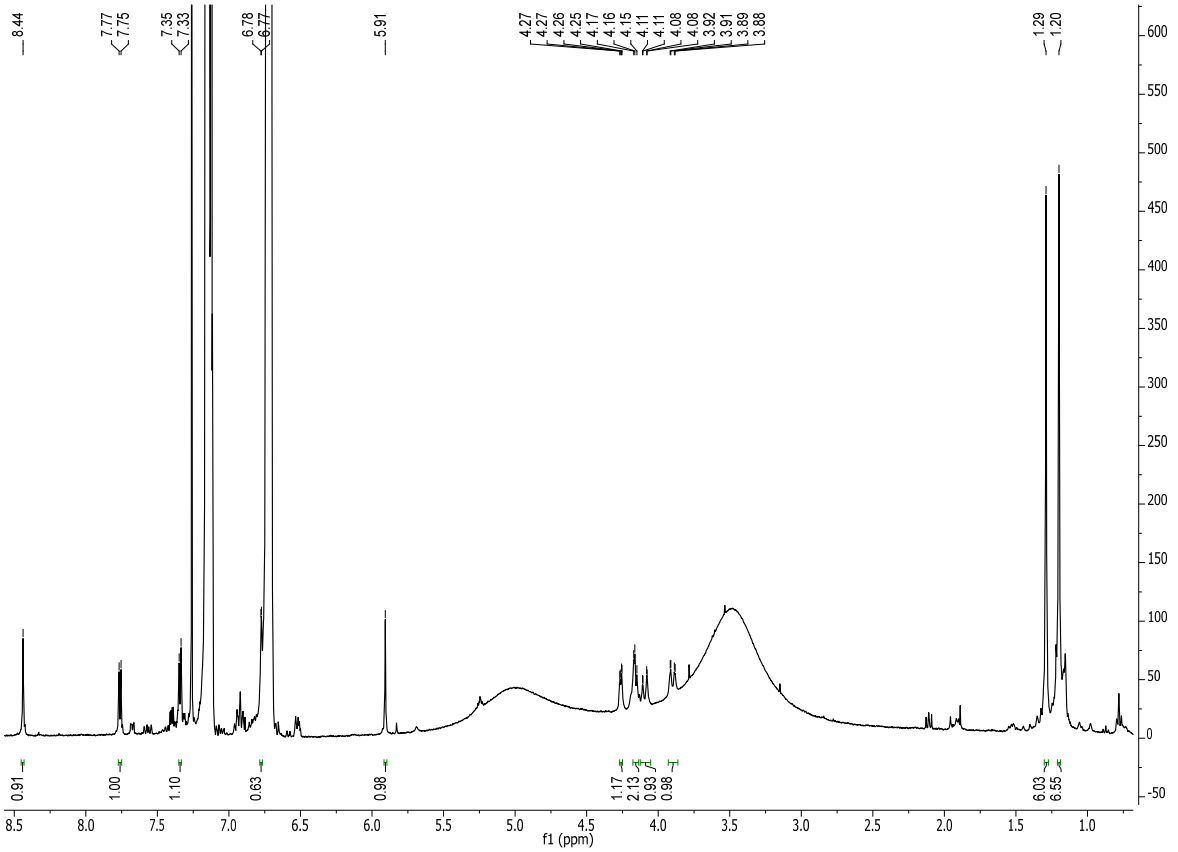

^{31}P-NMR spectrum of compound **2** (D_2O, 162 MHz, r.t.)

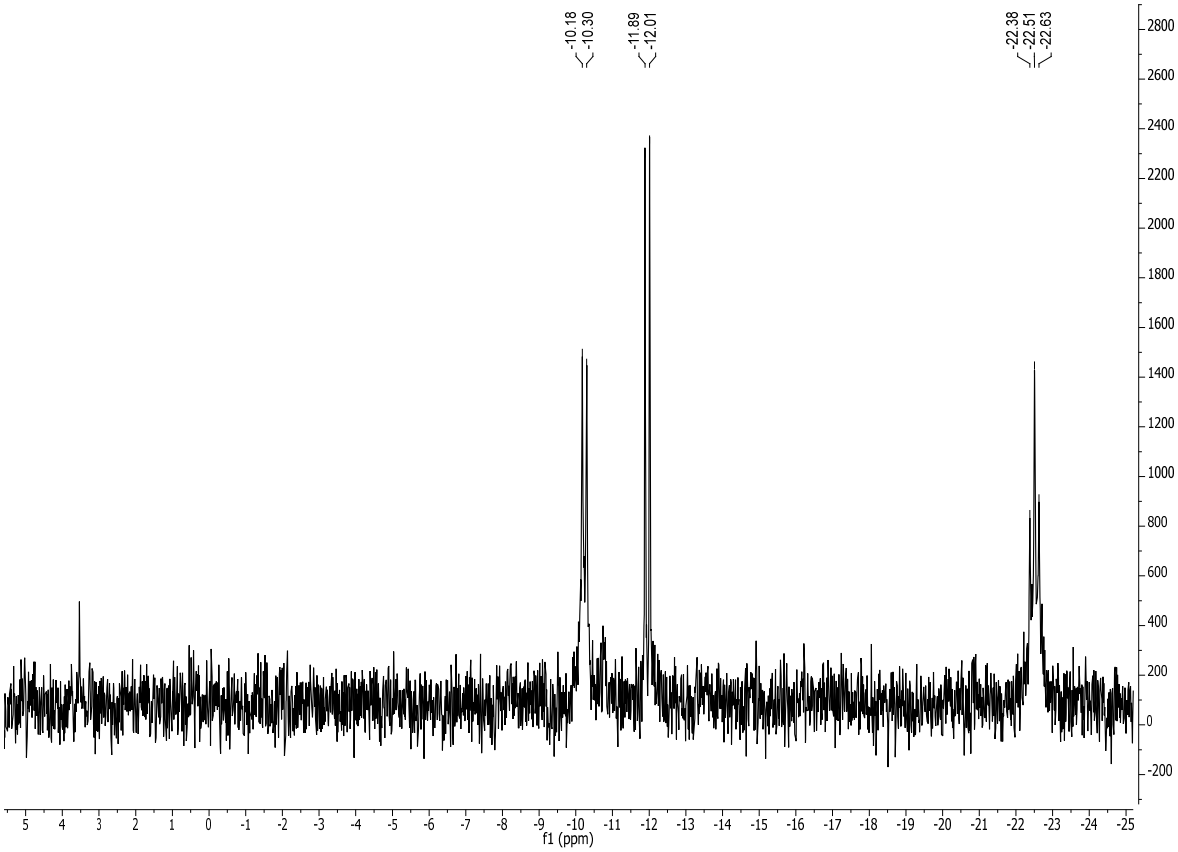

^{1}H-NMR spectrum of compound **2** (D_2O, 400 MHz, r.t.)

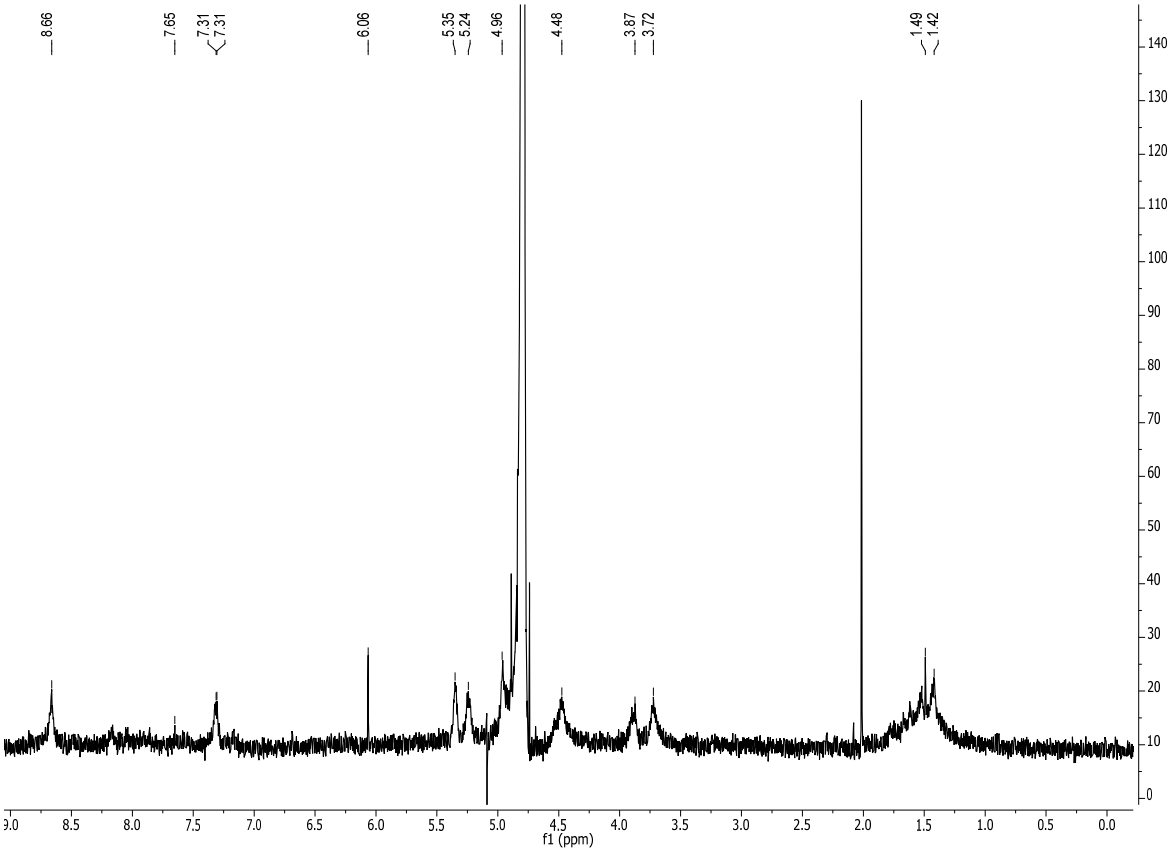

Mass spectra

Calculated (lower image) and high resolution ESI⁺ mass spectrum (upper image) of compound **5**.

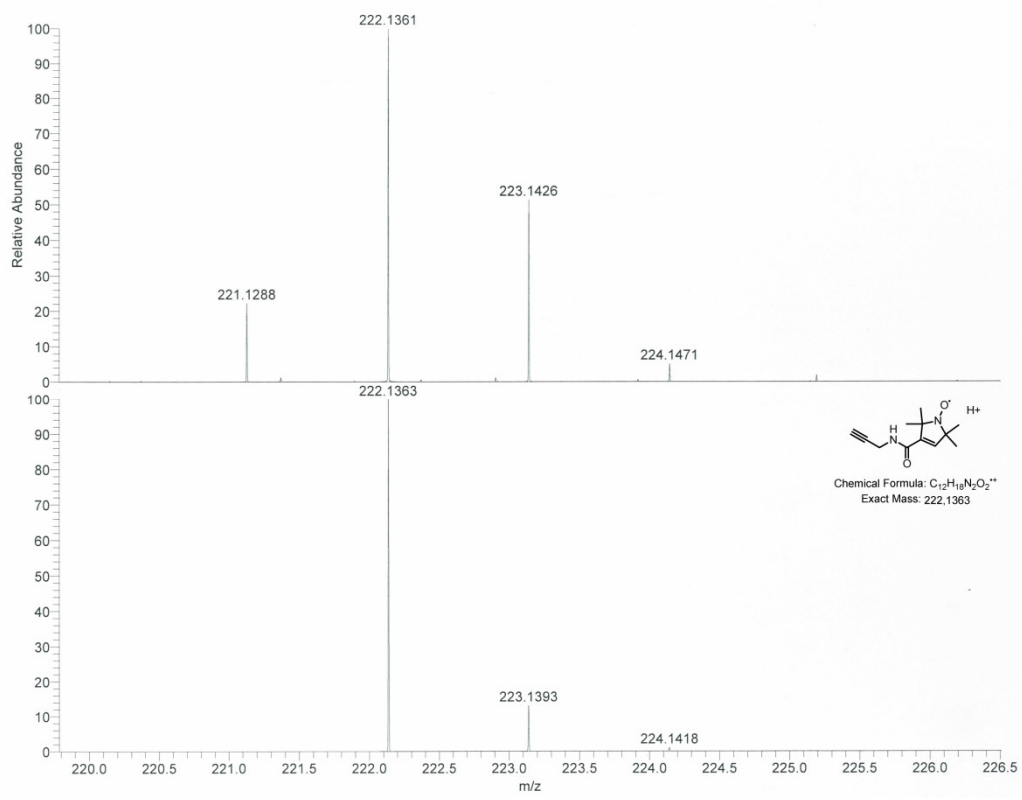

Calculated (lower images) and high resolution ESI⁺ mass spectrum (upper image) of compound **6**.

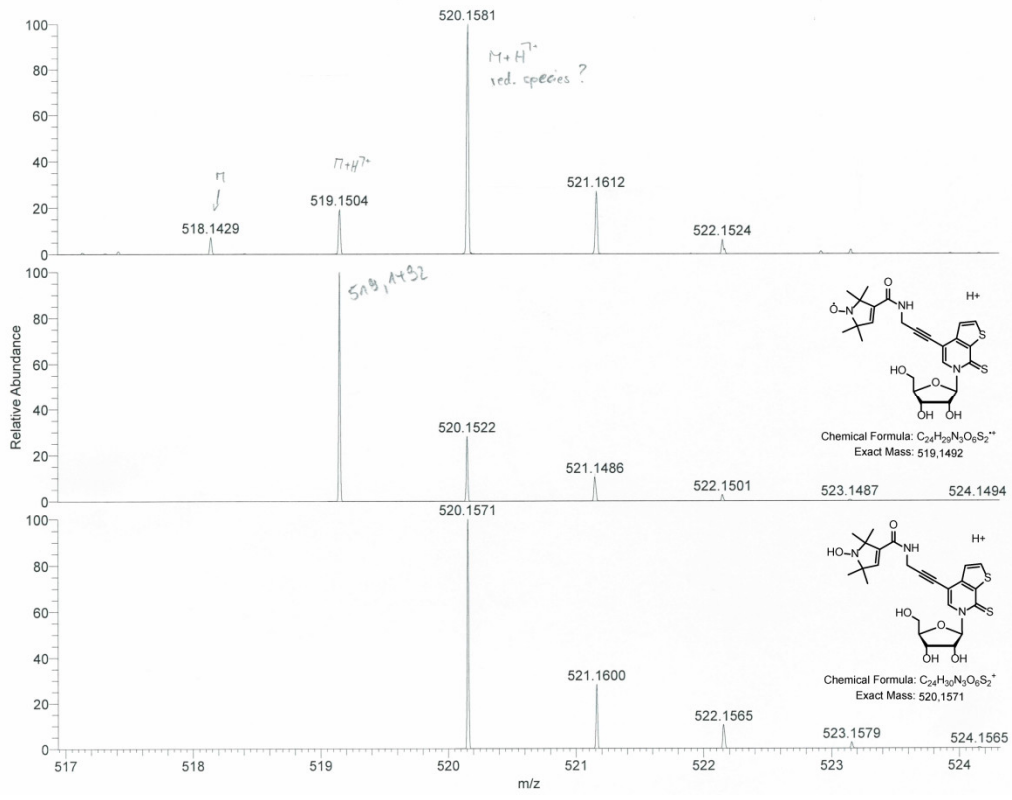

Calculated (lower image) and high resolution ESI$^+$ mass spectrum (upper image) of compound **1**.

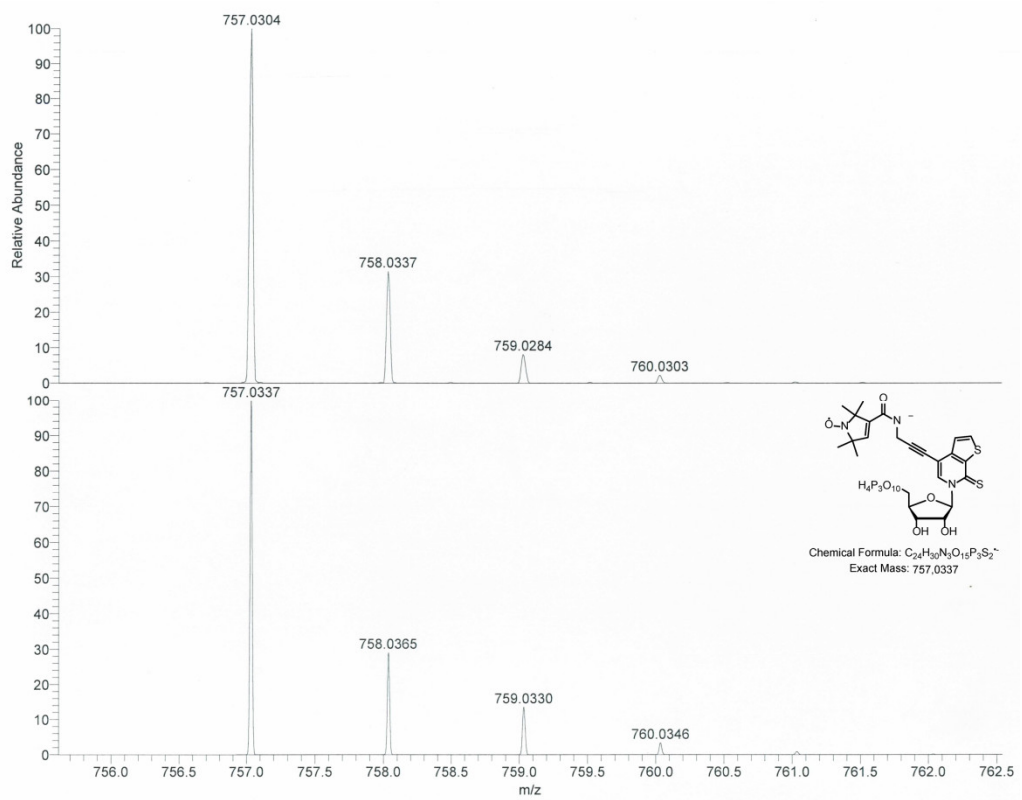

Calculated (lower image) and high resolution ESI$^+$ mass spectrum (upper image) of compound **8**.

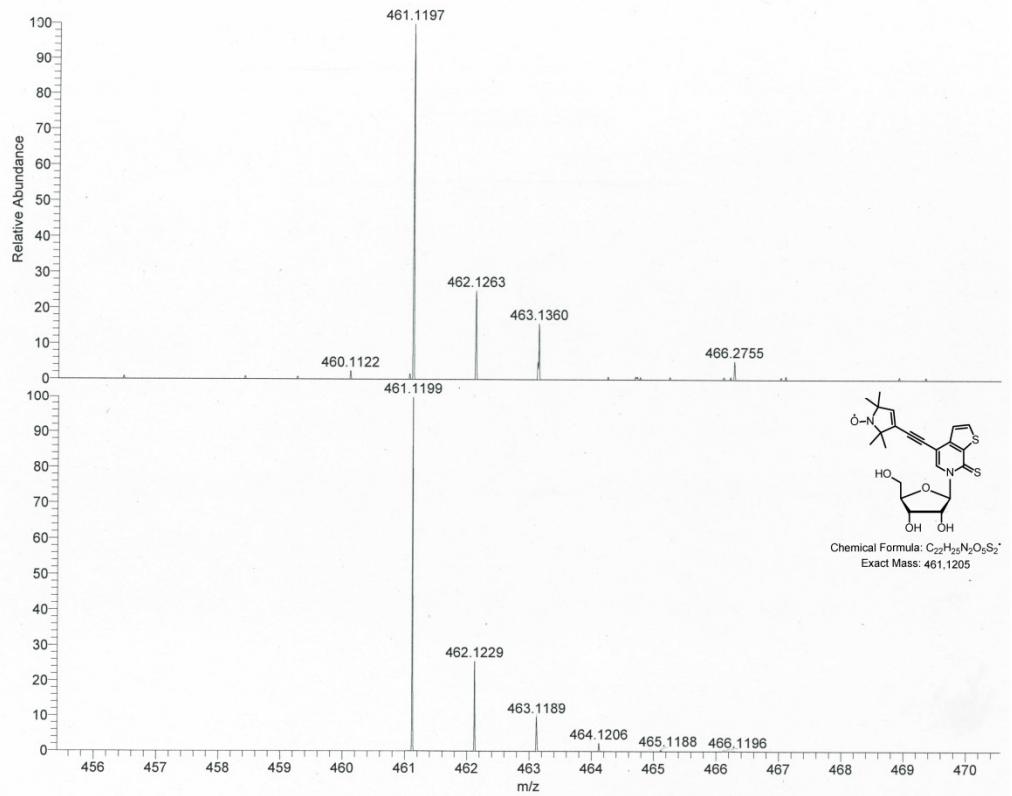

Calculated (lower image) and high resolution ESI$^+$ mass spectrum (upper image) of compound **2**.

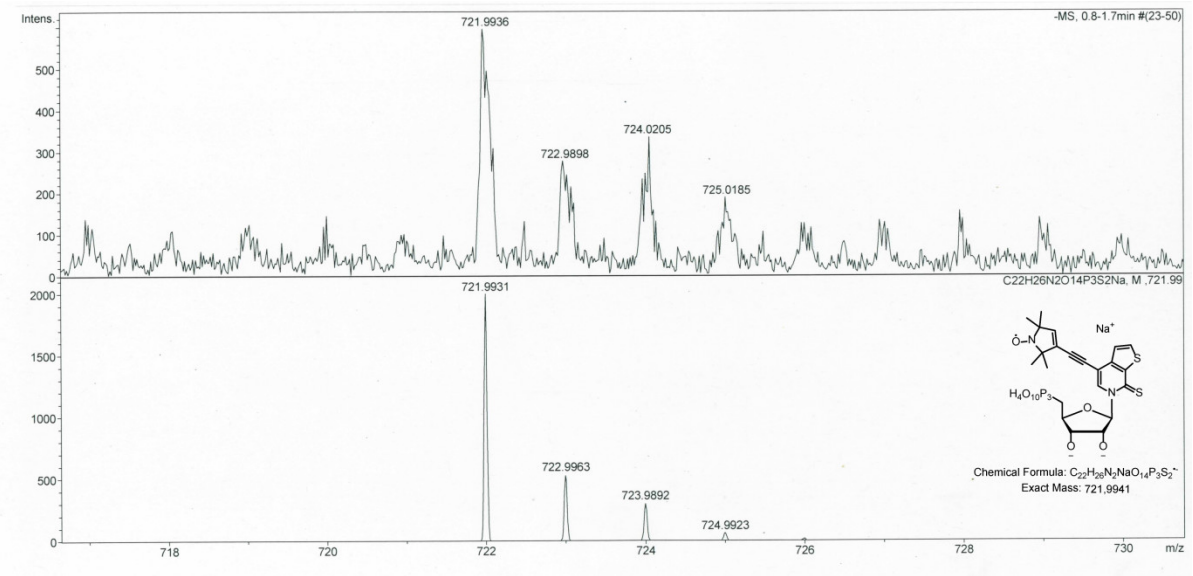

Literature

[1] G. R. Fulmer, A. J. M. Miller , N. H. Sherden, H. E. Gottlieb, A. Nudelman, B. M. Stoltz, K. I. Goldberg, *Organometallics* **2010**, *29* (9), 2176-2179.

[2] C. Domnick, F. Eggert, S. Kath-Schorr, *Chem. Commun.* **2015**, *51*, 8253-8256.

[3] O. Schiemann, N. Piton, J. Plackmeyer, B. E. Bode, T. F. Prisner, J. W. Engels, *Nature Protocols* **2007**, *2*, 904–923.

[4] S. Obeid, M. Yulikov, G. Jeschke, A. Marx, *Angew. Chem. Int. Ed.* **2008**, 47, 6782-6785.

[5] L. Li, M. Degardin, T. Lavergne, D. A. Malyshev,K. Dhami, P. Ordoukhanian,F. E. Romesberg, *J. Am. Chem. Soc.* **2014**, *136*, 826–829.

[6] Y. J. Seo, G. T. Hwang, P. Ordoukhanian, F. E. Romesberg, *J. Am. Chem. Soc.* **2009**, *131*, 3246–3252.

[7] D. A. Benson, I. Karsch-Mizrachi, D. J. Lipman, J. Ostell, D. L. Wheeler, GenBank. Nucleic Acids Research, **2005**, *33* (Database Issue), D34–D38. http://doi.org/10.1093/nar/gki063

[8] G. Jeschke, V. Chechik, P. Ionita, A. Godt, H. Zimmermann, J. Banham, C. Timmel, D. Hilger, H. Jung, *Appl. Magn. Reson.* **2006**, *30*, 473-498.

[9] CGenFF:

a) A. K. Vanommeslaeghe, E. Hatcher, C. Acharya, S. Kundu, S. Zhong, J. Shim, E. Darian, O. Guvench, P. Lopes, I. Vorobyov, A. D. MacKerell Jr., *J. Comput. Chem.* **2010**, 31, 671-690.

b) B. W. Yu, X. He, K. Vanommeslaeghe, A. D. MacKerell Jr., *J. Comput. Chem.* **2012**, 33, 2451-2468.

c) H. Yu, Y. Mu, L. Nordenskiold and G. Stock, *J Chem Theory Comput.,* **2008**, *4*, 1781-1787.

d) K. Vanommeslaeghe, A. D. MacKerell Jr., *J. Chem. Inf. Model.* **2012**, *52*, 3144-3154.

e) K. Vanommeslaeghe, E. P. Raman, A. D. MacKerell Jr., *J. Chem. Inf. Model.* **2012**, *52*, 3155-3168.

f) CGenFF interface at paramchem.org: https://cgenff.umaryland.edu

[10] CHARMM

a) R. B. Best, X. Zhu, J. Shim, P. E. Lopes, J. Mittal, M. Feig and A. D. Mackerell, Jr., J *Chem Theory Comput.* **2012**, *8*, 3257-3273.

b) Denning, E.J., Priyakumar, U.D., Nilsson, L., and MacKerell Jr., A.D., *J Comput. Chem.* **2011**, *32,* 1929-43.

c) E. Prabhu Raman, Justin A. Lemkul, Robert Best, Alexander D. MacKerell, Jr., CHARMM36 port: http://mackerell.umaryland.edu/charmm_ff.shtml

[11] Gromacs:

a) H. J. C. Berendsen, D. van der Spoel, R. van Drunen, *Computer Physics Commun.,* **1995**, *91*, 43-56.

b) D. van der Spoel, E. Lindahl, B. Hess, G. Groenhof, A. E. Mark and H. J. C. Berendsen, *J. Comp. Chem.* **2005**, *26*, 1701-1719

c) S. Pronk, S. Páll, R. Schulz, P. Larsson, P. Bjelkmar, R. Apostolov, M. R. Shirts, J. C. Smith, P. M. Kasson, D. van der Spoel, B. Hess, E. Lindahl, *Bioinformatics* **2013**, *29*, 845-54

d) M. J. Abraham, T. Murtola, R. Schulz, S. Páll, J. C. Smith, B. Hess, E. Lindahl, *SoftwareX* **2015**, *1*, 19-25.

[12] C. Domnick, G. Hagelueken, F. Eggert, O. Schiemann, S. Kath-Schorr, *Org. Biomol. Chem.* **2019**, *17*, 1805-1808.